*Advances in Civil Engineering*

RESEARCH ARTICLE OPEN ACCESS

# Prediction of Mechanical Properties of Spent Coffee Ground Ash Mixed Asphalt Using Experimental Investigation and Machine Learning Approaches

Shiva Kumar G.[1] | Doma Hemanth Kumar[1] | M. S. Ujwal[1] | Raghavendra Mahesh[1] | H. K. Ramaraju[1] | Poornachandra Pandit[2]

[1]Department of Civil Engineering, Dayananda Sagar College of Engineering, Bengaluru 560111, India | [2]Manipal Institute of Technology, Manipal Academy of Higher Education, Manipal 576104, India

**Correspondence:** Poornachandra Pandit (pc.pandit@manipal.edu)

**Received:** 24 November 2025 | **Revised:** 21 May 2026 | **Accepted:** 13 June 2026

**Academic Editor:** Shikha Binwal

**Keywords:** machine learning | pavement performance | SHAP analysis | spent coffee ground ash | sustainable asphalt mixtures

## ABSTRACT

This study investigates the feasibility of utilizing spent coffee ground ash (SCGA) as a sustainable bio-modifier for asphalt binders and mixtures through an integrated experimental and computational framework. The novelty of this research lies in the adoption of a dual-strategy approach that combines comprehensive experimental validation with explainable artificial intelligence (XAI) for predictive performance assessment. Unlike previous investigations that focused separately on binder-level or mixture-level behavior, the present study integrates laboratory characterization, mechanical performance evaluation, machine learning prediction, and SHAP-based interpretability within a single unified framework. SCGA was incorporated at dosages of 2%, 4%, 6%, and 8% by weight of binder to evaluate its effects on physical, rheological, durability, and mechanical properties of asphalt mixtures. Experimental investigations included penetration, softening point, viscosity, storage stability, Marshall stability, indirect tensile strength (ITS), tensile strength ratio (TSR), rutting resistance, fatigue performance, and ultrasonic pulse velocity (UPV) assessments. Results demonstrated that SCGA significantly enhanced binder stiffness and high-temperature performance, with penetration decreasing by 21% and viscosity increasing by nearly 49% relative to the control binder (CB). The optimum performance was achieved at 6% SCGA, where Marshall stability increased by 19%, ITS improved by 10%, rutting resistance increased by ~12%, and fatigue life (FL) improved by nearly 12% compared with the conventional mixture. However, excessive SCGA content (8%) reduced moisture resistance and fatigue performance because of increased brittleness and excessive stiffening. To strengthen predictive capability, decision tree and XGBoost regression models were developed, where the decision tree model achieved superior prediction accuracy with an $R^2$ value of 0.98. Furthermore, SHAP analysis identified ITS and modulus-related parameters as the most influential factors governing asphalt mixture performance, demonstrating the effectiveness of XAI in supporting sustainable pavement material design and engineering decision-making. This study highlights SCGA as a promising eco-friendly additive for enhancing the properties of asphalt pavement, contributing to Sustainable Development Goals (SDGs) 9 (Industry, Innovation, and Infrastructure), 11 (Sustainable Cities and Communities), 12 (Responsible Consumption and Production), and 13 (Climate Action).

This is an open access article under the terms of the Creative Commons Attribution License, which permits use, distribution and reproduction in any medium, provided the original work is properly cited.

Copyright © 2026 Shiva Kumar G. et al. *Advances in Civil Engineering* published by John Wiley & Sons Ltd.

## 1 | Introduction

Flexible pavements constitute the most widely adopted form of roadway infrastructure worldwide, primarily because of their cost-effectiveness, ease of construction, adaptability to staged development, and simple maintenance compared with rigid pavements [1, 2]. In developing countries such as India, flexible pavements dominate the highway network, which accounts for more than 85% of the total passenger traffic and nearly 65% of the total freight traffic [3–5]. However, their structural performance and durability are continuously limited by increasing traffic volume, heavier axle load, and varying climatic conditions. Common distresses such as rutting, fatigue cracking, thermal cracking, and moisture-induced damage limit service life and increase the financial burden of frequent rehabilitation [6, 7]. Since the mechanical behavior of flexible pavements is highly dependent on the properties of the bituminous binder, research has long focused on binder modification strategies to increase resistance to temperature susceptibility, oxidative aging, fatigue, and deformation [8]. The demand for sustainable, high-performance materials in pavement engineering has therefore accelerated the exploration of alternative additives and modifiers to improve durability while reducing the industry's environmental footprint. In recent years, the global drive toward sustainability in civil engineering has created opportunities to incorporate industrial and agricultural byproducts into asphalt pavements [9]. Such approaches aim to reduce dependency on virgin petroleum-based products while valorizing wastes that would otherwise contribute to environmental degradation [10, 11]. Among these byproducts, spent coffee ground ash (SCGA) has attracted increasing attention because of the sheer magnitude of global coffee waste generation and its potential for beneficial reuse. More than 10 million tons of coffee waste are produced worldwide each year, most of which ends up in landfills, where it causes soil contamination, methane emissions, and other negative environmental effects [12]. Transforming this waste into SCGA through controlled combustion not only addresses pressing waste management challenges but also provides a material with chemical characteristics suitable for construction applications [13]. Thus, its use in flexible pavements contributes directly to circular economy practices, resource efficiency, and long-term sustainability [14].

SCGA is rich in silica, alumina, iron oxides, and other mineral constituents comparable to those found in established supplementary cementitious materials such as fly ash, rice husk ash, and bagasse ash [15]. These chemical and physical properties make SCGA a promising filler or modifier for bituminous binders and mixtures. Studies have reported that SCGA can improve mixture stability, stiffness, and aging resistance while also positively influencing moisture susceptibility and fatigue life (FL) under controlled dosages. When used as a mineral filler in hot-mix asphalt, SCGA has favorable effects on mechanical strength and binder aggregate bonding, thereby extending the pavement service life [16, 17]. Furthermore, combustion and thermogravimetric analyses of SCGA have provided insights into its thermal stability, fusibility, and ash formation behavior, which are critical for high-temperature pavement applications in regions with warm climates [18]. Beyond its role as an ash, innovative approaches have explored SCGA in combination with other industrial byproducts to maximize its effectiveness. For example, hybrid mixtures of SCGA with fly ash or limestone filler have demonstrated synergistic effects, resulting in enhanced stiffness, moisture resistance, and overall durability [19]. Additionally, SCGA has been associated with beneficial modifications in binder rheology, including improvements in penetration resistance, softening point, ductility, and viscosity. These improvements are directly linked to the fine particle size and reactive oxides present in SCGA, which act to densify the asphalt matrix, improve mastic cohesion, and enhance binder aggregate interactions [20, 21]. investigated the use of coffee husk ash as a mineral filler in hot-mix asphalt and reported improvements in mechanical stability and moisture resistance. In contrast [22], employed coffee husk ash as a cementitious binder replacement and reported decreases in strength and workability, thereby limiting its acceptable replacement level to 10% cement [23]. utilized coffee husks as a partial sand replacement in concrete and reported a decrease in compressive strength [24]. incorporated spent coffee ground (SCG) oil into asphalt binders and reported the restoration of linear viscoelastic behavior in aged binders along with enhanced resistance to permanent deformation [5]. evaluated SCG as a biobased binder modifier at dosages ranging from 5% to 15% by weight of bitumen; the incorporation of SCG increased binder stiffness and slightly improved aging resistance, leading to the recommendation of an optimal SCG content of 5% by weight of bitumen [4]. modified asphalt binders using SCG in powder and ash forms and assessed their physical and rheological properties. The inclusion of SCG reduced the penetration and ductility values, indicating increased binder stiffness, whereas improvements in rutting and fatigue resistance were observed. Furthermore, compared with the SCG powder, the SCGA demonstrated superior high-temperature performance. Collectively, these findings highlight the versatility of SCGA and its potential to serve multiple functions in sustainable pavement engineering, ranging from being a mineral filler to being a performance-enhancing biomodifier [25–27].

Despite these advances, the current body of literature has notable limitations. Many studies have examined SCGA in isolated contexts, focusing on either binder-level or mixture-level performance, without integrating both scales in a unified experimental framework [28]. While mechanical improvements have been reported, the systematic optimization of SCGA dosage remains underexplored [29]. Excessive replacement levels can adversely affect binder workability, increase brittleness, and disrupt mixture compaction, whereas insufficient dosages may fail to yield measurable improvements [30]. Moreover, the majority of existing studies have relied exclusively on laboratory experimentation, with limited integration of computational modeling techniques to predict and generalize the performance across multiple parameters [29]. This restricts the practical applicability of research findings and limits the development of performance-based design guidelines for field implementation [31–33]. The primary objective of the present study is to evaluate the feasibility of using SCGA as a sustainable modifier in asphalt binders and mixtures, with an emphasis on optimizing mechanical performance while addressing environmental concerns associated with coffee waste disposal [34]. Research has systematically investigated the effects of SCGA on binder properties, including penetration, softening point, ductility, viscosity, and storage stability, as well as on mixture-level parameters, such as Marshall stability, the tensile strength ratio (TSR), FL, rutting resistance, and the resilient modulus (rapid rutting [RR]) [35–38]. By linking binder- and mixture-level performance,

this study develops a comprehensive understanding of the role of SCGA in modifying asphaltic materials. In addition to experimental investigations, this work integrates machine learning approaches to improve predictive accuracy and support engineering decision-making [30, 39–42]. Specifically, decision tree and XGBoost models are employed to predict performance parameters on the basis of experimental datasets. To ensure interpretability, SHapley Additive exPlanations (SHAP) analysis is used to identify the relative importance of input features, providing transparency into the influence of SCGA dosage, binder properties, and mixture characteristics [43]. This dual-strategy experimental validation coupled with explainable artificial intelligence (XAI) represents a methodological advancement over previous works that relied solely on laboratory testing. The novelty of this research lies in its combined experimental–computational framework [44, 45]. Unlike earlier works that considered SCGA in isolation, this study integrates binder characterization, mixture performance, and machine learning-based predictive modeling into a single coherent investigation [46, 47]. This approach not only validates the feasibility of the SCGA in improving the durability and sustainability of flexible pavements but also demonstrates the role of XAI in strengthening engineering decision-making [47–52]. Ultimately, the outcomes of this work contribute to advancing sustainable pavement technologies, valorizing abundant agricultural byproducts, and promoting environmentally responsible infrastructure development [53–61]. Table 1 compares recent recent biomass–ash studies and present work. Unlike previous biomass-ash asphalt studies that focused primarily on laboratory performance evaluation, the present research integrates experimental testing with explainable machine learning to develop a decision-support framework [65–67]. Rather than relying solely on statistical regression, the proposed approach identifies governing mechanical predictors such as ITS and modulus through SHAP analysis, enabling a mechanistic interpretation of asphalt mixture behavior and improving performance-based design [68, 69].

## 2 | Methodology of the Present Work

A comprehensive approach that combines experimental investigations with machine learning models to explore the suitability of SCGA as an environmentally friendly component in asphalt mixtures is illustrated in Figure 1. This integrative framework not only examines material performance through laboratory tests but also leverages predictive analytics to assess its long-term viability and potential benefits for sustainable road construction. The process begins with the procurement of raw materials, including aggregates, bitumen, and SCGs, which are processed to obtain SCGA in proportions of 2%–8%. Bitumen characterization through penetration, softening point, ductility, viscosity, storage stability, and flash point tests is carried out to ensure the suitability for blending. The SCGA was then incorporated into the mix design, and samples were prepared for laboratory testing. The performance parameters studied include the TSR, rutting resistance, fatigue resistance, dynamic modulus (DM), and elastic modulus (EM), offering comprehensive insights into the mechanical performance of asphalt mixtures. In addition, microstructural analysis is performed to examine the bonding and interaction of SCGA with the asphalt matrix at the microscopic level. Parallel to the experimental program, the generated data undergo refinement and preparation for the machine learning phase. Predictive models are developed using decision tree regression and XGBoost algorithms, with datasets divided for training and validation. Their predictive performance and interpretability are evaluated through Taylor diagrams, REC curves, SHAP values, and feature importance rankings. This integrated methodology combines experimental results with computational modeling, ensuring reliability, generating predictive insights, and validating SCGA as a sustainable, high-performing material for asphalt pavement design.

## 3 | Materials and Testing Protocol

### 3.1 | Materials

Granite aggregates (coarse and fine) were procured from local quarry sources and used in this study in accordance with MoRTH specifications for bituminous concrete (BC). The adopted aggregate gradation satisfied the permissible limits for BC Grade 2 mixtures, confirming a well-graded aggregate skeleton suitable for asphalt mixture preparation (Figure 2). To improve clarity and technical organization, this section systematically presents material sources, physical properties, and SCGA microstructural characterization through concise tables and figures, including SEM and EDS analyses, thereby reducing the descriptive text while enhancing readability. The engineering properties of aggregates were evaluated using standard IS 2386 procedures, and the results confirmed their suitability for pavement applications. The results are tabulated in Table 2.

SCGs collected from local coffee outlets were processed to obtain SCGA. Initially, the coffee residues were oven-dried at $105 \pm 5°C$ for 24 h to remove moisture. The dried residues were then subjected to controlled calcination in a muffle furnace at 600°C for 4 h, ensuring the complete removal of volatile components, oils, and carbonaceous matter. This thermal treatment yielded a stable ash with a more defined mineral composition suitable for use in asphalt mixtures. A muffle furnace with a heating rate capacity of 5°C per minute was used to obtain the SCGA. It was held at the

**TABLE 1** | Comparison of recent biomass-ash asphalt studies and present work.

| Study | Material | Method | ML used | Key limitation |
|---|---|---|---|---|
| [21] | Coffee husk ash | Experimental only | No | No predictive framework |
| [62] | Wood ash asphalt filler | Experimental | No | Limited mechanistic insight |
| [63] | RAP Rejuvenated asphalt | Regression + ML | ANN/SVM | No interpretability |
| [64] | Asphalt mixtures | ML prediction | Multiple models | No experimental integration |
| Present study | SCGA asphalt | Experimental + ML + SHAP | DT + XGBoost | — |

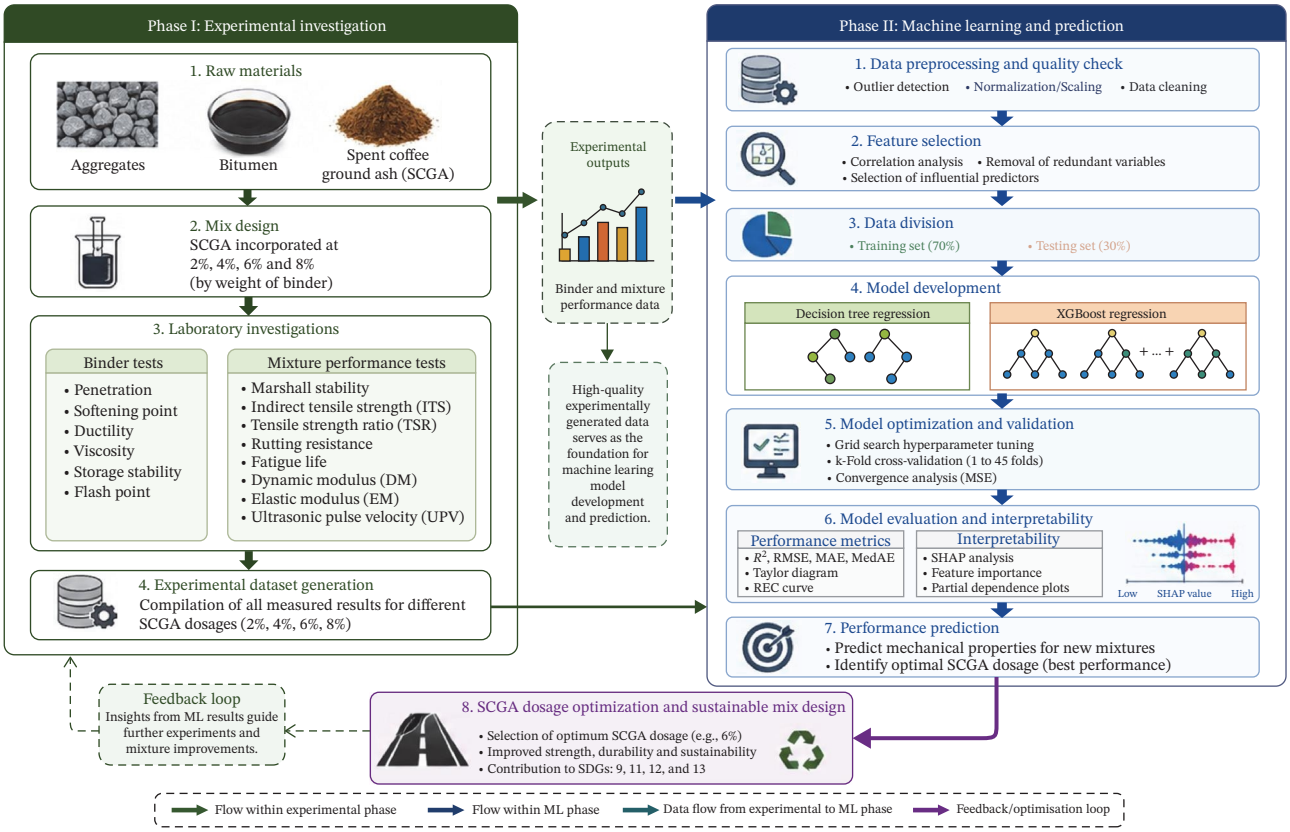



**FIGURE 1** | Methodology of the experiments and ML.

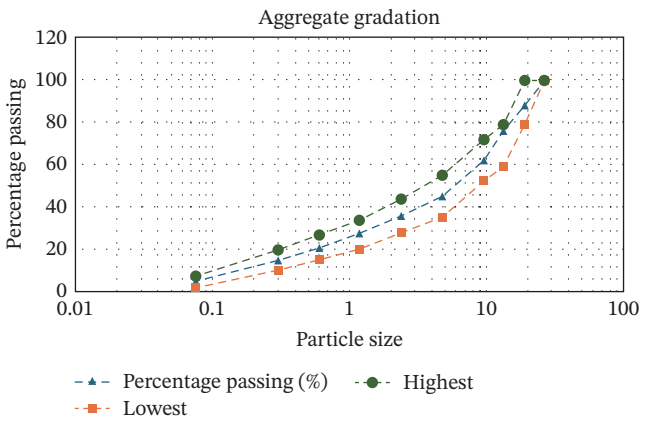



**FIGURE 2** | Aggregate gradation curve compared with MoRTH specification limits for BC grade 2 mixtures.

**TABLE 2** | Physical properties of aggregates.

| Property | Test standard | Value | Specification limits |
|---|---|---|---|
| Los Angeles abrasion | IS 2386 (Part 4) | 19% | Max. 30% |
| Aggregate impact value | IS 2386 (Part 4) | 17% | Max. 24% |
| Water absorption | IS 2386 (Part 3) | 0.11% | Max. 2% |
| Flakiness + elongation index | IS 2386 (Part 1) | 25% | Max. 35% |
| Soundness | IS 2386 (Part 5) | 0.3% | Max. 12% |

target temperature for 3 h and then allowed to reach room temperature. Previous studies have commonly adopted a calcination temperature of ~550°C for SCGA preparation [4, 22, 46]. In the present study, a slightly higher temperature of 600°C was selected to promote enhanced pore development while retaining sufficient surface activity, which is expected to improve interfacial adhesion with the asphalt binder and facilitate greater bitumen absorption [48]. Increasing the calcination temperature within this range generally enhances pore development while reducing ash reactivity [39]. The SCGA physical characteristics are shown in Table 3.

Granite aggregates used in this investigation were procured from local quarry sources and satisfied the MoRTH specifications for BC Grade 2 mixtures. The aggregate gradation was maintained within the specified limits to ensure proper interlocking, stability, and load distribution in asphalt mixtures. Engineering properties including Los Angeles abrasion value, aggregate impact value, water absorption, flakiness and elongation index, and soundness were evaluated according to IS 2386 standards. The obtained results confirmed adequate resistance to wear, impact, and

**TABLE 3** | SCGA physical characteristics.

| Property | Value |
|---|---|
| Calcination temperature | 600°C |
| Calcination duration | 4 h |
| Specific gravity | 0.75 |
| Mean particle size (D50) | 30 μm |

weathering, thereby demonstrating the suitability of the aggregates for pavement applications. SCGs collected from local coffee outlets were processed to produce SCGA. The collected residues were initially oven-dried at 105 ± 5°C for 24 h to remove moisture and subsequently calcined in a muffle furnace at 600°C for 4 h to eliminate volatile compounds and organic matter. This controlled calcination process produced a stable ash possessing a porous morphology and mineral-rich characteristics suitable for asphalt modification. The selected calcination temperature enhanced pore development and improved the surface characteristics of SCGA, thereby increasing its interaction with the asphalt binder.

The physical appearance of SCGA is presented in Figure 3a, where the ash appears as a fine dark-gray powder with lightweight characteristics because of its low specific gravity and porous internal structure. To further evaluate the microstructural characteristics, scanning electron microscopy (SEM) and energy-dispersive spectroscopy (EDS) analyses were performed. The SEM micrograph shown in Figure 3b reveals irregular, angular, rough, and porous particles with non-uniform sizes and interconnected voids formed during calcination. Such a porous morphology increases the specific surface area, thereby enhancing binder absorption, internal friction, and aggregate–binder interaction. Consequently, improved stiffness and rutting resistance of asphalt mixtures can be achieved. The EDS spectrum presented in Figure 3c confirms the presence of major elements, including oxygen (O), calcium (Ca), potassium (K), carbon (C), silicon (Si), aluminum (Al), and magnesium (Mg). The oxide-rich mineral phases formed during calcination contribute to improved filler reactivity, adhesion, stiffness enhancement, and microstructural densification. Overall, the combined SEM–EDS analysis confirms that SCGA possesses favorable morphological and chemical characteristics suitable for use as a sustainable bio-modifier and microfiller in asphalt mixtures.

## 3.2 | Specimen Preparation

To alter the SCGA, a paving-grade unmodified asphalt binder (VG-30) was used as a control binder (CB). The necessary amount of SCGA was added to the hot CB over the course of approximately 10 minutes to create the modified binder with SCGA. The mixture was mixed at 700 rotations per minute for 2 h, while the temperature was maintained at 160–170°C. The modified binders prepared using 2%, 4%, 6%, and 8% SCGA were designated SCGA2, SCGA4, SCGA6, and SCGA8, respectively. The dosage range adopted in this study was based on evidence from prior literature investigating SCGA in asphalt binders [4]. evaluated SCGA and SCG in powder form over a dosage range of 1%–8% by wt. of bitumen, whereas [5] used SCGA contents of 5%–15%, recommending an optimal dosage of ~5% on the basis of rheological performance. Considering these findings, in the present study, a conservative and practically relevant dosage range of 2%–8% was selected. The physical properties, viscosity, and storage stability of the modified and CBs were tested.

## 3.3 | Experimental Methods

The effects of various SCGA dosages (2%, 4%, 6%, and 8%) were evaluated by a battery of assays at the binder and combination levels. For unaged conventional binder (CB) and modified binders containing 2%, 4%, 6%, and 8% SCGA, the penetration, softening point, ductility, and flash point of the typical binder tests were conducted in the context of the Indian paving grade (IS 1201–1220). Using a Brookfield rotating viscometer in accordance with ASTM D4402, the viscosity at 135°C was measured to evaluate the workability. Storage stability tests were performed to evaluate the stability of modified binders during storage in terms of the separation or segregation of modifiers or additives. To assess this as per IRC SP 53 (2023), the modified bitumen, which is stored and sealed in aluminium tubes, is kept in a hot oven at 163°C in the vertical position for 48 h. The softening point was determined for binder samples at the top and bottom portions, and the variation in the softening point was used to indicate the storage stability. The Marshall mix design, as per Asphalt Institute (1996), was adopted to determine the optimum binder content (OBC) and to prepare the asphalt mixture samples for further evaluation of their mechanical properties. Marshall samples 100 mm in diameter were compacted such that 75 blows per side were used, as per MoRTH (2013). The volumetric properties of the mixtures, such as voids in the total mixture (VTM), voids in mineral aggregates (VMA), voids filled with asphalt (VFA), and bulk density (Gmb), were determined.

Indirect tensile strength (ITS) and RR tests were used to evaluate moisture damage and rutting resistance, respectively, on cylinders with 7.0 ± 0.1% air space. The ITS test procedure is adopted as per ASTM D6931. After conditioning the samples for 1 h at 50°C in the ITS setup, rutting was measured, and the TSR was computed in accordance with AASHTO T283. For both the control and SCGA-modified mixtures, the rutting resistance was measured in terms of rutting strength (kPa). This method allowed a direct assessment of the effect of SCGA on the ability of the mixtures to resist plastic flow under sustained loading, thereby providing valuable insights into the optimum dosage required to enhance pavement performance against permanent deformation. The fatigue resistance of the asphalt mixtures was evaluated using the ITS test. The TSR,

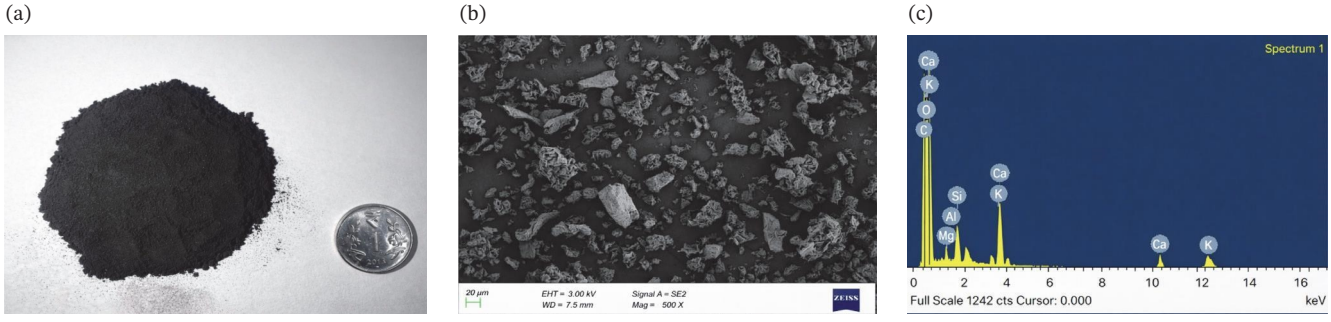



**FIGURE 3** | (a) Spent coffee ground ash, (b) microscopy image, and (c) chemical composition.

which was computed as the ratio of the tensile strength of the conditioned sample to that of the unconditioned sample in accordance with AASHTO T283, was used to assess the moisture resistance of the mixes. Three replicate samples were prepared for each test, and the average of those samples is reported in this study. The fatigue strength was evaluated using the repeated load testing method in accordance with [45, 47]. Cylindrical HMA samples were subjected to cyclic diametrical loading, with a loading duration of 0.1 s, followed by a rest period of 0.9 s, corresponding to a loading frequency of 1 Hz. The cyclic load was continuously applied until the sample reached a predefined failure criterion of 5 mm of vertical deformation. The total number of loading cycles sustained by the sample at the point of failure was recorded and reported as the FL. The control combination and mixtures made with the SCGA2, SCGA4, SCGA6, and SCGA8 binders underwent fatigue testing. Ten percent of the tensile strength of the control mixture (CM) was applied regularly during fatigue testing until a 5 mm deformation was observed. The transmitter and receiver were positioned parallel to the destructive load to measure the velocity of the ultrasonic pulses on the cylindrical samples. A 50 kHz transducer was used to test an air void sample with an asphalt concentration of $4.0 \pm 0.1\%$. Furthermore, the elastic and dynamic moduli of the mixtures were assessed.

## 4 | Machine Learning

Traditional regression models are typically limited to capturing linear relationships between variables and may not adequately represent the complex interactions among stiffness, tensile strength, and durability parameters that govern asphalt mixture behavior. In contrast, machine learning algorithms such as decision tree and XGBoost are capable of modeling nonlinear dependencies and hierarchical feature interactions, enabling more accurate representation of the multivariate relationships inherent in asphalt materials. Although several parameters exhibit strong pairwise correlations, correlation-based or simple regression approaches cannot fully describe the combined influence of multiple mechanical variables acting simultaneously. The proposed machine learning framework allows the simultaneous prediction of multiple performance indicators by learning the nonlinear relationships among the tensile strength, modulus, FL, and moisture resistance parameters. In addition, SHAP analysis enhances interpretability by quantifying the relative contribution of interacting features, thereby extending beyond conventional correlation analysis and supporting performance-oriented decision-making in asphalt mixture design. Such an approach reduces the reliance on iterative experimental trials while maintaining strong predictive reliability and engineering transparency.

### 4.1 | Data Preparation and Preprocessing

The machine learning framework adopted in the present study was developed to evaluate the predictive capability of decision tree and XGBoost regression models for estimating the mechanical and durability properties of SCGA-modified asphalt mixtures. The experimental dataset incorporated key asphalt performance parameters including Marshall stability, ITS under dry and wet conditions (ITS dry and ITS wet), TSR, resilient modulus (RR), FL, dynamic modulus (DM), and elastic modulus (EM). These parameters collectively represent the strength, stiffness, moisture resistance, deformation resistance, and long-term durability behavior of asphalt mixtures containing SCGA.

Initially, the developed machine learning framework included several experimentally measured mechanical parameters as input variables to investigate the statistical interrelationships among asphalt mixture properties and evaluate the capability of the models to capture coupled mechanical behavior. However, because many of these parameters are physically interconnected, the simultaneous use of these variables as both input features and prediction targets may introduce multicollinearity and information leakage, potentially leading to artificially inflated prediction accuracy and unrealistic model performance. Therefore, the predictive framework was revised to improve scientific consistency, practical applicability, and generalization capability. In the revised framework, only independent mixture design and material-related variables, including bitumen content (BC), SCGA dosage, and other physically independent descriptors, were used as input features for model development. The experimentally measured mechanical properties such as stability, ITS dry, ITS wet, TSR, RR, FL, DM, and EM were treated exclusively as target outputs and were not simultaneously used as predictors for one another. This revised strategy minimizes information leakage and ensures that the developed models predict asphalt mixture performance solely on the basis of independent material and mixture design parameters rather than previously known mechanical outputs.

The dataset used in this investigation consisted of 120 experimentally generated samples obtained through controlled laboratory investigations on SCGA-modified asphalt mixtures. Prior to model implementation, systematic preprocessing and quality verification procedures were carried out to ensure the reliability and consistency of the dataset. The data were examined for missing values, duplicate records, abnormal observations, and inconsistencies associated with laboratory measurements. Since all samples were generated under controlled conditions, no missing values were identified, and all experimental observations were verified using the original laboratory records. Additional statistical range verification and correlation analysis were also conducted to ensure that the measured values remained within physically realistic limits for asphalt mixtures. The Decision Tree and XGBoost models were subsequently trained using randomized train–test splitting integrated with k-fold cross-validation and grid-search hyperparameter optimization. Preliminary exploratory analyses also included Random Forest regression; however, the final predictive framework presented in the article includes only the Decision Tree and XGBoost models. Therefore, all REC curves, Taylor diagrams, figure captions, and corresponding discussions were revised to remove residual references to Random Forest and maintain consistency throughout the article. The revised machine learning framework represents a scientifically reliable and physically consistent predictive approach for evaluating the performance of SCGA-modified asphalt mixtures. The integration of independent material-related input variables, robust validation strategies, and multiple statistical performance indices significantly improves the reliability, interpretability, and generalization capability of the developed models for predicting the mechanical behavior of sustainable asphalt mixtures under unseen conditions.

## 4.2 | Data Splitting and Training Testing Strategy

The machine learning framework developed in the present study was designed to evaluate the predictive capability of decision tree and XGBoost regression models for estimating the mechanical and durability properties of SCGA-modified asphalt mixtures. The complete experimental dataset consisted of 120 laboratory-generated samples obtained from asphalt mixtures containing varying dosages of SCGA. The collected data included key performance parameters such as Marshall stability, ITS under dry and wet conditions (ITS dry and ITS wet), TSR, RR, FL, DM, and EM, which collectively represent the strength, stiffness, deformation resistance, and durability characteristics of asphalt mixtures. Before model implementation, systematic preprocessing and quality verification procedures were performed to ensure consistency and reliability of the dataset. The experimental data were examined for missing values, duplicate entries, abnormal observations, and inconsistencies associated with laboratory measurements. Since the dataset was generated under controlled laboratory conditions, no missing records were identified, and all observations were verified using the original experimental data. Statistical range verification and correlation analysis were also performed to ensure that the measured values remained within physically realistic limits for asphalt mixtures.

Initially, the machine learning framework incorporated several experimentally measured mechanical properties as input variables to investigate the statistical interrelationships among asphalt mixture parameters and evaluate the capability of the developed models to capture coupled mechanical behavior. However, because parameters such as stability, ITS, TSR, modulus, and FL are physically interconnected, their simultaneous use as both inputs and outputs may introduce multicollinearity and information leakage, potentially leading to artificially inflated prediction accuracy. Therefore, the predictive framework was revised to improve scientific consistency and generalization capability. In the revised framework, only independent mixture design and material-related parameters, including BC, SCGA dosage, and other physically independent descriptors, were used as input features for model development, whereas the mechanical properties were treated exclusively as target outputs. This revised approach minimizes information leakage and improves the practical applicability and physical interpretability of the developed models. The dataset was subsequently divided into independent training and testing subsets to evaluate the predictive capability and generalization performance of the models. Several train–test combinations, including 60:40, 70:30, 75:25, and 80:20 ratios, were examined through sensitivity analysis to identify the most suitable data distribution strategy. Among these combinations, the 70:30 split demonstrated the most balanced performance in terms of prediction stability, model consistency, and unbiased evaluation of unseen data. Consequently, 84 samples (70%) were randomly allocated for model training and hyperparameter optimization, whereas the remaining 36 samples (30%) were reserved exclusively for independent testing and validation. The testing samples were not used during training, feature selection, hyperparameter tuning, or cross-validation procedures, thereby ensuring unbiased model evaluation.

To further improve robustness and minimize overfitting, k-fold cross-validation was incorporated during model development. The primary reason for adopting k-fold validation was the relatively limited dataset size of 120 samples. When only a single proportional train–test split is used, the predictive performance may become highly dependent on the selected training and testing samples, leading to instability and prediction bias. The k-fold cross-validation technique overcomes this limitation by systematically dividing the dataset into multiple folds, where each subset is used once for validation, while the remaining folds are used for training. This approach ensures that every sample contributes to both training and validation stages, thereby improving statistical reliability and reducing sensitivity to data partitioning. In addition, the k-fold convergence analysis was extended up to 45 folds to evaluate the stability and convergence behavior of the developed models under progressively increasing validation partitions. The convergence plots demonstrated that both decision tree and XGBoost models achieved stabilization of MSE values at higher folds, confirming improved prediction consistency and reduced sensitivity to data partitioning.

## 4.3 | Performance Indices

Since the present study focuses on the regression-based prediction of continuous asphalt mixture performance parameters, classification-oriented evaluation tools such as precision–recall curves and confusion matrices were not applicable. Instead, regression-based statistical indicators were adopted to assess the model accuracy, error magnitude, and overall predictive reliability. Model performance was evaluated using four complementary metrics: the coefficient of determination ($R^2$), mean squared error (MSE), root mean square error (RMSE), and mean absolute error (MAE). The $R^2$ value quantifies the proportion of variance explained by the model, reflecting the strength of agreement between the predicted and experimental results. Error-based metrics such as MSE and RMSE emphasize larger deviations and are particularly useful for identifying models sensitive to significant prediction errors, whereas the MAE provides an intuitive measure of the average absolute deviation in the same units as the target variable. Together, these indices offer a comprehensive and balanced assessment of model performance, ensuring a reliable evaluation of prediction accuracy and generalization capability across different asphalt mixture parameters.

### 4.3.1 | RMSE

The RMSE represents the standard deviation of the residuals, which are the differences between the predicted and actual values. It is obtained by calculating the square root of the mean of the squared errors. Since the RMSE places a stronger emphasis on larger discrepancies, it is particularly sensitive to outliers. A smaller RMSE reflects superior model accuracy and improved predictive capability.

### 4.3.2 | Median Absolute Error

The MSE measures model accuracy by averaging the squared differences between actual and predicted outcomes. Like RMSE, it penalizes larger errors more heavily, which makes it highly responsive to substantial deviations. However, because MSE values are expressed in squared terms, their scale can be less straightforward to interpret, although the metric remains effective for evaluating and comparing different models.

#### 4.3.3 | MAE

The MAE represents the average of the absolute differences between the predicted and actual values. Unlike metrics that square the errors, the MAE provides a direct and easily interpretable measure of the typical prediction error, expressed in the same units as the dependent variable. In comparison to the RMSE, it is less affected by extreme values, making it a more robust indicator when outliers are present.

#### 4.3.4 | $R^2$ Score

The coefficient of determination ($R^2$) expresses the proportion of variance in the dependent variable that can be explained by the independent variable(s). Its value ranges from 0 to 1, where 1 represents a perfect fit, while a value close to 0 indicates that the model offers little improvement over simply using the mean of the dependent variable. Together with $R^2$, the error-based metrics provide additional insights: the RMSE and MSE emphasize larger deviations, making them suitable for comparing models with respect to significant errors, whereas the MAE conveys the average prediction error in an easily interpretable form. By integrating these complementary measures, a holistic evaluation of each model's ability to predict the compressive strength of concrete can be achieved.

### 4.4 | Overfitting Prevention and Generalization Capability

Several measures were implemented during model development to minimize curve-fitting (overfitting) effects and improve the generalization capability of the developed machine learning framework. For the decision tree model, tree depth limitation, minimum sample split constraints, minimum leaf sample requirements, and pruning conditions were applied to control excessive model growth and reduce memorization of training data. Similarly, for the XGBoost model, regularization parameters, learning rate optimization, subsampling ratios, and boosting constraints were incorporated to improve robustness and reduce overfitting sensitivity. In addition, randomized train–test splitting and k-fold cross-validation ensured repeated validation of the models using previously unseen data. Multiple statistical indices including $R^2$, RMSE, MAE, RSR, NSE, PI, and a20-index were simultaneously considered to evaluate prediction reliability rather than relying solely on high correlation values. Although the developed decision tree model achieved high prediction accuracy, its applicability to completely unknown datasets should be interpreted within the investigated parameter range and material conditions. Since the experimental dataset was generated under controlled laboratory conditions, the developed models are expected to provide reliable predictions for asphalt mixtures possessing similar material characteristics, SCGA dosage ranges, and testing conditions. Further validation using larger field-scale datasets may improve the broader generalization capability of the proposed framework.

### 4.5 | Machine Learning Models

Decision tree and XGBoost models were selected because of their ability to capture nonlinear relationships among mixture parameters while maintaining interpretability and computational efficiency for relatively small experimental datasets. Decision trees provide transparent rule-based predictions that facilitate engineering interpretation, whereas XGBoost incorporates boosting and regularization mechanisms that enhance the predictive robustness and generalizability. Compared with more complex ensemble approaches such as random forest, which may reduce interpretability and introduce additional variance for limited datasets, the selected models offer a balanced combination of accuracy, transparency, and computational stability suitable for engineering applications characterized by strong physical correlations among variables. Model development followed a structured optimization workflow to ensure reliable performance and minimize overfitting. The hyperparameters for both the decision tree and XGBoost models were tuned using a grid-search strategy integrated with k-fold cross-validation, allowing the systematic exploration of model configurations while validating the performance across multiple dataset partitions. For the XGBoost model, key parameters, including the learning rate (0.05–0.3), maximum tree depth (3–8), number of estimators (50–200), and subsampling ratio (0.7–1.0), were evaluated. Similarly, decision tree parameters such as maximum depth, minimum number of samples per split, and minimum number of samples per leaf were optimized to balance the model complexity and prediction accuracy. Tree-pruning constraints were applied to prevent excessive model growth and reduce sensitivity to dataset-specific patterns. In addition to hyperparameter optimization, feature importance assessment was performed using SHAP analysis and correlation mapping to interpret input–output relationships and identify the governing mechanical variables influencing asphalt mixture performance. This integrated workflow ensured that the final models achieved strong predictive capability while maintaining physical interpretability and robustness against overfitting.

#### 4.5.1 | Decision Tree Regression

Decision tree regressors operate by dividing the input space into regions defined by feature-based splits, aiming to minimize the mean-squared error within each partition. Unlike models that rely on gradient descent for optimization, decision trees use a greedy strategy, selecting the best split at each step. These split points effectively serve as model parameters, guiding how predictions are made within each subset of the data.

#### 4.5.2 | XG Boost Regression

XGBoost is an advanced ensemble learning technique that uses gradient boosting to increase the accuracy and efficiency by building on the concept of decision trees. Instead of creating trees independently as in random forests, XGBoost builds its model in a sequential manner, where each new tree is designed to correct the residual errors of the preceding ensemble. It employs gradient descent optimization to update parameters, allowing each subsequent tree to place greater emphasis on the samples that were more difficult to predict in earlier iterations. This iterative refinement enhances both the accuracy and robustness of the overall model. To maintain high performance while balancing model complexity and predictive accuracy, a regularized objective function is employed. The overall prediction is produced by combining the outputs of all the trees in the ensemble, with each tree contributing a weighted score. These cumulative contributions form the

**TABLE 4** | ML model and its equation.

| Sl. No | Parameter | Equation |
|---|---|---|
| 1 | Root mean square error (RMSE) | $\mathrm{MSE} = \sqrt{\frac{1}{n}\sum_{i=1}^{n}(y_i - \widehat{y}_i)^2}$ |
| 2 | Median absolute error (MedAE) | $\mathrm{MedAE} = \mathrm{median}(\lvert y_i - \widehat{y}_i \rvert)$ |
| 3 | Mean absolute error (MAE) | $\mathrm{MAE} = \frac{1}{n}\sum_{i=1}^{n}\lvert y_i - \widehat{y}_i \rvert$ |
| 4 | $R^2$ score | $R^2 = 1 - \frac{\sum_{i=1}^{n}(y_i - \widehat{y_i})^2}{\sum_{i=1}^{n}(y_i - \bar{y})^2}$ |
| 5 | Decision tree regression | $\widehat{y} = \sum_{m=1}^{M} c_m I(x \in R_m)$ |
| 6 | XGBoost regression | $\widehat{y}_i = \sum_{k=1}^{K} f_k(x_i), \quad f_k \in F$ |

*Note:* $y_i$ represents the experimental value, $\widehat{y}_i$ denotes the predicted value, $\bar{y}$ is the mean of the observed values, $n$ represents the total number of samples, $c_m$ denotes the predicted output in region $R_m$, and $I(x \in R_m)$: is the indicator function used in decision tree regression. In the XGBoost equation, $f_k$ represents the individual regression trees combined through boosting to generate the final prediction.

final model output, enabling more accurate and reliable predictions. Table 4 shows the ML model and its equations.

#### 4.5.3 | Hyperparameter Optimization and Model Configuration

To improve the predictive capability, robustness, and generalization performance of the developed machine learning framework, hyperparameter optimization was performed for both the decision tree and XGBoost regression models (Table 5). The optimization process was carried out using a grid-search strategy integrated with k-fold cross-validation to systematically determine the optimal combination of hyperparameters while minimizing overfitting and prediction uncertainty. The final hyperparameter configurations were selected based on the combinations that produced the highest prediction accuracy together with the lowest RMSE and MAE values on the validation dataset.

For the decision tree regression model, parameters controlling tree growth and structural complexity were optimized to improve prediction stability and avoid excessive model branching. The maximum tree depth was adjusted to prevent overfitting to the experimental dataset, whereas the minimum number of samples required for node splitting and leaf node formation was optimized to reduce sensitivity to noise within the laboratory-generated data. The optimized decision tree configuration demonstrated strong capability in capturing the nonlinear relationships among the asphalt mixture performance parameters while maintaining reduced computational complexity and low prediction uncertainty.

Similarly, for the XGBoost Regression model, several boosting and regularization parameters including the learning rate, maximum tree depth, number of estimators, subsampling ratio, and column sampling ratio were optimized. The learning rate controlled the contribution of each boosting iteration and improved convergence stability, while the number of estimators governed the boosting stages during model development. Subsampling and feature sampling ratios improved model generalization and reduced the dependency on specific training samples or variables. Regularization parameters were also incorporated to minimize excessive model complexity and reduce overfitting sensitivity. The optimized decision Tree model demonstrated comparatively lower RMSE, MAE, and RSR values together with higher $R^2$ and NSE values for most of the investigated performance parameters. This behavior can be attributed to the structured nature of the experimental dataset and the strong nonlinear relationships among the mechanical properties of SCGA-modified asphalt mixtures. Although the XGBoost model exhibited slightly higher prediction errors, its boosting and regularization mechanisms improved generalization capability and stability across different dataset partitions. Overall, the integration of grid-search optimization and k-fold cross-validation significantly enhanced the reliability,

**TABLE 5** | Optimized hyperparameter configuration of machine learning models.

| Model | Hyperparameter | Optimized value | Purpose |
|---|---|---|---|
| Decision tree | Maximum depth | 5 | Controls tree complexity and prevents overfitting |
| | Minimum samples split | 2 | Minimum samples required for node splitting |
| | Minimum samples leaf | 1 | Controls leaf node size and stability |
| | Criterion | Squared error | Minimizes prediction error |
| XGBoost | Learning rate | 0.1 | Controls boosting contribution |
| | Maximum depth | 4 | Balances flexibility and generalization |
| | Number of estimators | 100 | Number of boosting iterations |
| | Subsample ratio | 0.8 | Improves robustness and reduces overfitting |
| | Column sample ratio | 0.8 | Reduces feature dependency |
| | Regularization alpha | 0.01 | Controls model complexity |
| | Regularization lambda | 1.0 | Prevents excessive overfitting |

robustness, and engineering applicability of the developed machine learning models.

The correlation heatmap (Figure 4) provides valuable insights into the relationships among the different performance parameters of the bituminous mixtures. The color scale ranges from dark purple, representing weak or negative correlations (close to –0.2) to bright yellow, representing very strong positive correlations (approaching +1). The BC is moderately positively correlated with the TSR ($r = 0.55$), resilient modulus (RR, $r = 0.35$), and FL ($r = 0.47$), whereas it is very weakly or slightly negatively correlated with the stability (ST, $r = –0.094$) and SCGA (SC, $r = –0.02$). The SCGA content generally shows negligible or weak correlations, with most values close to zero, except for a slight positive relationship with RR ($r = 0.26$) and a weak negative relation with TSR ($r = –0.15$), suggesting that its influence on mechanical properties is more indirect. Stability is strongly correlated with dry ITS (ITSD, $r = 0.94$), RR ($r = 0.74$), FL ($r = 0.69$), deformation ($r = 0.77$), and EM ($r = 0.78$), highlighted in yellow tones, confirming that stability is tightly linked with overall strength and stiffness properties. ITSD is strongly correlated with EM ($r = 0.92$), deformation ($r = 0.86$), and RR ($r = 0.86$), whereas ITSW (wet strength) is strongly correlated with EM ($r = 0.95$), FL ($r = 0.93$), and deformation ($r = 0.91$), emphasizing that moisture resistance directly influences durability and stiffness. TSR is strongly dependent on ITSW ($r = 0.76$) and FL ($r = 0.67$), with moderate ties to BC ($r = 0.55$). The RR also strongly correlated with the ITSD ($r = 0.86$), FL ($r = 0.83$), deformation ($r = 0.82$), and EM ($r = 0.82$), reflecting its critical role in predicting long-term performance. The FL has the highest correlation with EM ($r = 0.96$), followed by ITSW ($r = 0.93$) and ITSD ($r = 0.83$), forming a bright-yellow cluster that highlights the dependance of endurance on strength and stiffness. Similarly, deformation is strongly correlated with ITSW ($r = 0.91$), ITSD ($r = 0.86$), and EM ($r = 0.90$), indicating that rutting resistance is largely governed by the tensile strength and modulus. Overall, the heatmap indicates a strong interdependency among ST, ITSD, ITSW, EM, FL, RR, and DM, forming a highly correlated group represented by bright yellow shades, whereas BC shows only moderate influence and SCGA remains weakly correlated, implying that its role is more subtle in enhancing performance characteristics.

## 5 | Results and Discussion

### 5.1 | Experimental

#### 5.1.1 | Conventional Bitumen Tests

Table 5 presents the physical and rheological properties of the CB and asphalt binders modified with various percentages of SCGA. The penetration and softening point test results reveal that incorporating SCGA enhances the high-temperature performance of the material and simultaneously decreases its sensitivity to

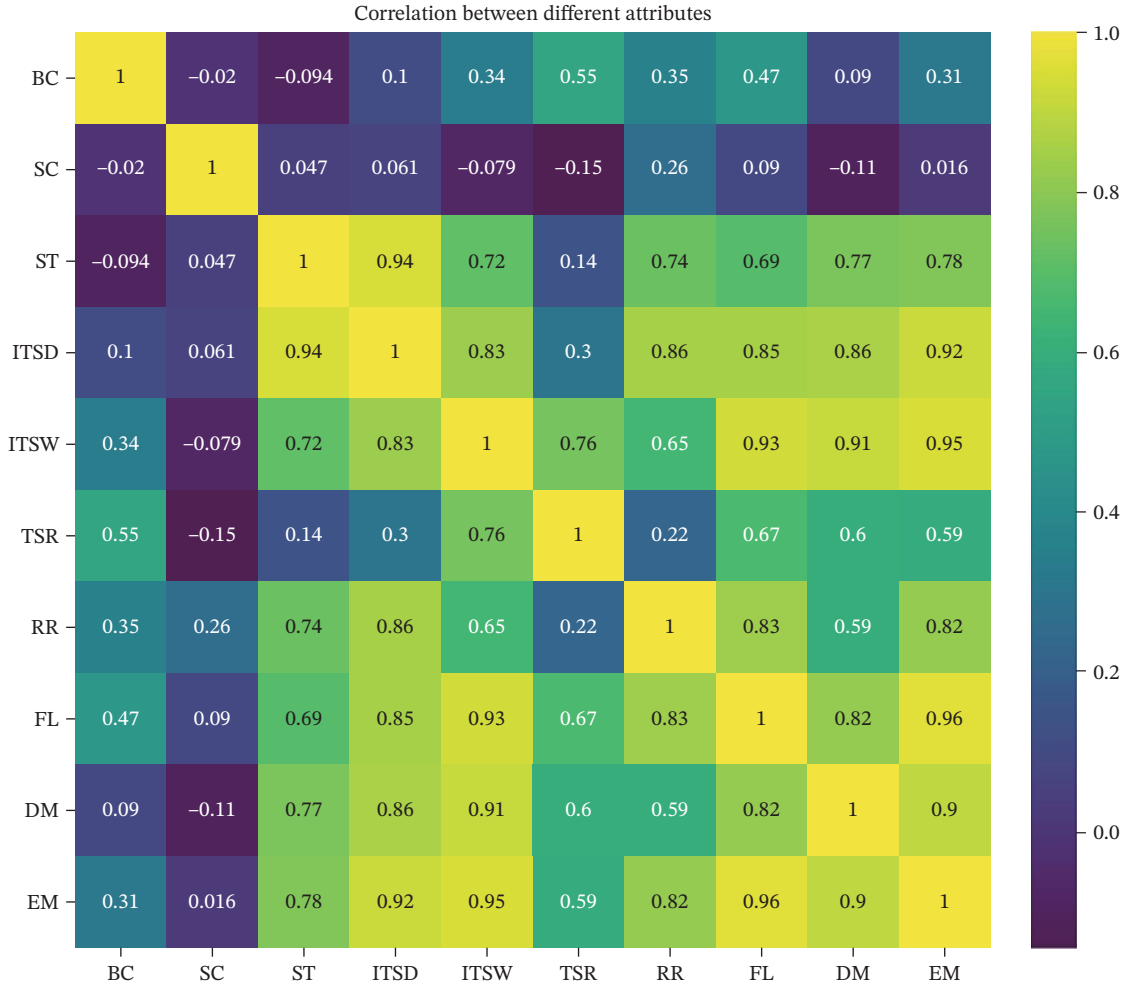



**FIGURE 4** | Correlation map.

temperature variations. An increase in the softening point indicates improved consistency or stiffness of the binder. The ductility of the asphalt binders decreases with increasing SCGA content, indicating reduced low-temperature performance. The reduced penetration values were also the same. As the content of SCGA increases, the flash point decreases, indicating reduced binder safety at high temperatures. The effects of SCGA replacement on the physical properties of bitumen. In Table 5, penetration decreases from 66 dmm (CB) to 52 dmm (SCGA8), indicating increased hardness, whereas the softening point increases from 49 to 55.3°C, reflecting improved temperature susceptibility. In Table 5, the ductility decreases from 130 cm (CB) to 70 cm (SCGA8), indicating decreased flexibility. The reduction in ductility from 130 to 70 cm upon SCGA incorporation can be attributed to the microstructural characteristics of SCGA observed in the SEM analysis. The particles exhibit an irregular morphology, angular edges, and porous surfaces, which act as rigid inclusions within the binder matrix. These features restrict molecular mobility, increase internal friction, and promote stress concentration during tensile deformation [70]. Additionally, the porous structure likely absorbs lighter maltene fractions, increasing the effective asphaltene content and further reducing the elongation capacity [71]. Consequently, the binder exhibits a stiffer and less deformable response, resulting in decreased ductility. Simultaneously, the flash point decreases from 330 to 260°C, suggesting reduced thermal stability. All modified binders in this study have flash points that are significantly higher than the average asphalt working temperatures (150–170°C) and remain higher than the minimum limitations of 220°C, as specified by IS 73 (2013). From an operational perspective, this reduction becomes more significant at higher SCGA dosages (≥6%), as there is a smaller margin between the limiting temperature and flash point. This may increase the vulnerability to prolonged exposure to high temperatures or localized overheating. SCGA contents of up to 6% retain sufficiently high flash points to ensure safe handling under controlled plant conditions. SCGA incorporation enhances stiffness and softening resistance but compromises ductility and the flash point, requiring a balance for practical applications.

#### 5.1.2 | Viscosity and Storage Stability Test

The viscosity of the CB (unaged) and binders modified with 2%, 4%, 6%, and 8% SCGA was evaluated at 135°C using a rotational viscometer. As illustrated in Table 6, incorporating SCGA into the binder led to a noticeable increase in viscosity. With increasing SCGA content, the viscosity increases from 355 mPa·s (CB) to 530 mPa·s (SCGA8), reflecting improved binder stiffness [72]. Viscosity values ranging from 0.257 to 0.348 Pa·s for 2%–6% SCGA-modified binders were reported, whereas [4] reported values between 0.2 and 0.3 Pa·s for 2%–8% SCGA. Similarly, [5] reported an increase in binder viscosity with increasing SCG dosage. The higher viscosity observed in the present study (up to 530 mPa·s, i.e., 0.53 Pa·s at 8% SCGA) follows the same increasing trend reported in previous studies. The variation in absolute values may be attributed to differences in the base binder grade, SCGA source, particle characteristics, and preparation methodology. Moreover, the storage stability improved from 0.3 to 1.6°C. SCGA makes the asphalt binder stiffer, resulting in higher viscosity. The higher viscosity values imply that higher working temperatures are needed for asphalt mixtures. The softening point difference (SPD) increased with increasing SCGA content. The SPD for the SCGA2, SCGA4, and SCGA6 mixes ranged from 0.3 to 0.9°C; upon further increasing to 8% SCGA, the SPD increased significantly. This finding indicates that the occurrence of phase separation is minimal; thus, the properties of modified binders do not change upon storage or transportation at higher temperatures.

#### 5.1.3 | Mix Design Properties

The mix design characteristics of asphalt mixtures incorporating different proportions of SCGA, including Gmb, VTM, VMA, and VFA, were evaluated to analyze their influence on volumetric properties and to identify the OBC. The corresponding results are summarized in Table 7. The CM had a Gmb value of 2350 kg/m$^3$. In comparison, mixtures incorporating 2%, 4%, 6%, and 8% SCGA (SCGA2, SCGA4, SCGA6, and SCGA8) presented Gmb values of 2355, 2358, 2365, and 2357 kg/m$^3$, respectively. The bulk density of the asphalt mixtures increased with increasing SCGA content. The optimal binder content (OBC) increased with increasing SCGA dosage. This can be attributed to the high surface area, low specific gravity, and porous nature of SCGA, which promote binder absorption and interfere with aggregate packing. This leads to an increase in the number of voids in the mineral aggregate. A higher binder content is necessary to properly cover the additional voids and ensure appropriate coating and cohesiveness within the asphalt matrix. The VMA increased with increasing SCGA, which aligned with the reduction in bulk density. Although the number of voids in the mineral aggregates increased, the number of VFA increased because of the potential improvement in the characteristics of the asphalt mixture.

#### 5.1.4 | ITS Test

ITS tests were conducted on both dry and moisture-conditioned samples to evaluate the cracking resistance and moisture susceptibility of the asphalt mixtures. The TSR, defined as the ratio of the conditioned strength to dry strength, was calculated, as shown in Table 8. For the CM, the TSR value was 93%, exceeding the

**TABLE 6** | Properties of conventional and SCGA-modified asphalt binders.

| Property | Penetration at 25°C, 0.1 mm | Softening point (°C) | Ductility at 25°C (cm) | Flash point (°C) | Viscosity (mPa•s) | Storage stability SPD (°C) |
|---|---|---|---|---|---|---|
| CB | 66 | 49 | 130 | 330 | 355 | NA |
| SCGA2 | 62 | 51 | 105 | 315 | 420 | 0.3 |
| SCGA4 | 58 | 53 | 95 | 295 | 460 | 0.6 |
| SCGA6 | 54 | 54 | 85 | 275 | 500 | 0.9 |
| SCGA8 | 52 | 55 | 70 | 260 | 530 | 1.6 |

**TABLE 7** | Asphalt mix design characteristics.

| Mix ↓ Units → | VTM (%) | OBC (%) | VMA (%) | VFB (%) | Gmb (kg/m$^3$) | Stability (kN) | Flow (mm) |
|---|---|---|---|---|---|---|---|
| CM | 4.0 ± 0.1 | 5.5 | 13.5 | 70.4 | 2350 | 10.5 | 3.0 |
| SCGA2 | | 6.2 | 14.0 | 71.4 | 2355 | 11.0 | 3.3 |
| SCGA4 | | 6.3 | 14.6 | 72.6 | 2358 | 11.6 | 3.7 |
| SCGA6 | | 6.4 | 15.2 | 73.7 | 2365 | 12.5 | 4.0 |
| SCGA8 | | 6.6 | 15.8 | 74.7 | 2357 | 11.5 | 4.4 |
| Requirement | 4.0 ± 0.1 | ≥5.4 | ≥13.0 | 65–78 | — | ≥9.0 | 2–4 |

**TABLE 8** | Indirect tensile strength, rapid rutting, and fatigue life results.

| Mix | ITS dry (kPa) | ITS wet (kPa) | TSR (%) | RR (kPa) | Fatigue life |
|---|---|---|---|---|---|
| CM | 650 | 605 | 93.1 | 630 | 13,800 |
| SCGA2 | 675 | 620 | 91.9 | 655 | 14,350 |
| SCGA4 | 690 | 630 | 91.3 | 670 | 14,890 |
| SCGA6 | 720 | 645 | 89.6 | 705 | 15,480 |
| SCGA8 | 670 | 560 | 83.6 | 650 | 12,950 |
| Requirement | — | ≥448 | ≥85% | — | — |

minimum threshold of 85% prescribed by AASHTO T283, thereby demonstrating sufficient resistance to moisture-induced deterioration. With the inclusion of SCGA, however, a reduction in TSR values was observed, signifying diminished moisture resistance of the modified mixtures. At 8% SCGA content, the TSR decreased to 83.6%, which falls below the permissible 85% limit, thereby rendering the mixture highly susceptible to moisture-induced stripping and durability issues. On the other hand, compared with those of the control, the dry ITS values clearly improved with SCGA addition, with increases ranging from 2.9% at lower dosages to 9.7% at higher dosages, reflecting enhanced cracking resistance under dry conditions. This contrasting behavior suggests that SCGA contributes to strengthening the binder–aggregate matrix in the absence of moisture by acting as a filler and improving the load distribution, whereas at higher contents, its porous and hydrophilic nature weakens the adhesive bond between the binder and aggregate in the presence of water, leading to reduced TSR. At an SCGA content of 8%, the TSR decreases considerably to 83.6%, approaching the AASHTO minimum requirement and suggesting increased sensitivity to moisture damage. This reduction is mostly attributed to the porous and absorptive characteristics of SCGA, which can lead to higher binder absorption and a reduction in the effective binder film thickness at the aggregate–binder interface [40, 73]. In addition, the comparably reduced surface polarity and chemical reactivity of SCGA at higher dosages may inhibit adhesive bonding, hence increasing the likelihood of moisture-induced damage. SCGA contents of up to 6% are considered acceptable from a durability standpoint because the related TSR values stay above the specification limits with a respectable margin of safety. Thus, although SCGA enhances tensile strength under dry conditions, its excessive incorporation, particularly at 8%, compromises the mixture's durability under moisture exposure, emphasizing the importance of optimizing its dosage for a balanced performance.

#### 5.1.5 | RR Test

RR test results clearly demonstrate the effect of SCGA on the rutting resistance of asphalt mixtures. The CM exhibited an RR value of 630 kPa, providing the baseline performance. With the incorporation of SCGA, a gradual improvement was noted up to the optimum dosage. At 2% SCGA, the RR value increased to 655 kPa, whereas at 4% SCGA, it further increased to 670 kPa, indicating that the addition of small amounts of SCGA improved the resistance of the mixture to permanent deformation. The maximum improvement was achieved at 6% SCGA, where the RR value reached 705 kPa, representing an 11.9% increase over the control. This enhancement is mainly linked to the filler role of the SCGA particles, which help minimize air voids, increase the mixture density, and improve the stiffness of the binder–aggregate matrix. Furthermore, the presence of mineral oxides in the ash strengthens binder–aggregate adhesion, thereby increasing the resistance of the mixture to rutting under repeated traffic loads. However, at 8% SCGA, the RR value decreased to 650 kPa, close to the control level, indicating a loss of the earlier improvements. This reduction can be explained by the excessive incorporation of SCGA, which disrupts the optimal gradation, increases brittleness, and creates weaker zones in the mastic, leading to reduced flexibility and higher susceptibility to microcracking under loading. Therefore, the results confirm that SCGA enhances rutting resistance up to an optimum dosage of ~6%, beyond which the negative effects of excess filler outweigh the benefits, highlighting the critical importance of dosage optimization for balancing stiffness and durability in asphalt mixtures.

#### 5.1.6 | Fatigue Test

The CMs and modified mixtures (SCGA2, SCGA4, SCGA6, and SCGA8) were subjected to repeated loading until the failure criterion of 5 mm deformation was met. The load corresponding to 10% of the failure load in the ITS test was applied, and the number of cycles corresponding to the failure criterion is reported in Table 7. The CM exhibited a FL of 13,800 cycles. The addition of spent coffee residue ash improved the fatigue of the asphalt mixtures. The FL of SCGA6 was 15480 cycles. When the amount of SCGA was further increased to 8%, the FL decreased. The fatigue resistance of the SCGA6 mixture increased, indicating that the FL increased, whereas the fatigue resistance of the SCGA8

mixture decreased. The progressive reduction in FL observed beyond a 6% SCGA content highlights the adverse effect of excessive stiffening on the cracking resistance of the mixture. This decline in performance is associated with increased brittleness and hardening of the asphalt binder caused by the higher proportion of SCGA. A similar trend can be observed for the ITS dry sample (Table 7). SCGA improves the tensile strength to some extent, but higher dosages have a negative effect on the tensile strength, leading to reduced fatigue resistance.

### 5.1.7 | Ultrasonic Pulse Velocity (UPV) Test

UPV tests were conducted in accordance with ASTM D5404 to assess the stiffness and elasticity of the bituminous mixtures. Dynamic and elastic moduli were determined from UPV data to indirectly evaluate the stiffness and elasticity, and higher moduli indicate better stiffness and elasticity. The test results are presented in Figure 5. The CM exhibited dynamic and elastic moduli of 31 and 11.8 GPa, respectively. The dynamic and elastic moduli of the SCGA increased to 6%, and a further increase in the SCGA content to 8% reduced the modulus from 14.1 to 11.2 GPa. With 6% SCGA (SCGA6), the DM increased to almost 5% compared with that of the CM, indicating improved tensile and elastic characteristics. On the other hand, SCGA8 with 8% SCGA exhibited the lowest dynamic and elastic moduli values of 30.5 and 11.2 GPa, respectively, indicating a reduced capacity to recover under repetitive loading. Although UPV-based modulus estimation offers valuable comparative insight into this stiffness–flexibility balance, the absolute modulus values must be interpreted cautiously because of their limitations. It may not capture the viscoelastic response of asphalt mixtures under traffic loading. The moduli are sensitive to the aggregate distribution and air void content, leading to variability. The mechanical properties improved up to 6% SCGA, and a further increase in the dosage of SCGA reduced the mechanical properties. This can be explained by the balance between mastic stiffness, binder availability, and interfacial integrity. At moderate SCGA dosages (up to 6%), SCGA primarily acts as a microfiller and reinforcing agent within the asphalt mastic. This leads to an increase in mastic stiffness because of the lower binder fractions without significantly lowering the effective binder content. This leads to an increase in both dynamic and elastic moduli, suggesting greater stiffness while maintaining sufficient flexibility. However, at higher dosages (8%) of SCGA, the balance is compromised because of the reduced effective binder film thickness, which hinders bonding between the binder and aggregate. This leads to brittle mastic and increased susceptibility to microcracking, which is reflected in reduced moduli. To improve the reliability and interpretability of the graphical results, error bars representing the standard deviation of triplicate experimental measurements have been incorporated into the mechanical and modulus-related plots, including the DM and EM trends. These error bars reflect the variability associated with sample preparation, air void distribution, and material heterogeneity, providing a clearer representation of the experimental uncertainty. Similarly, confidence bands derived from cross-validation residuals have been included in the prediction plots and Taylor diagram analyses to illustrate the dispersion of model outputs around the observed values. The relatively narrow confidence intervals observed for the stability, ITS, and modulus parameters confirm the consistency of the laboratory results and the robustness of the predictive models.

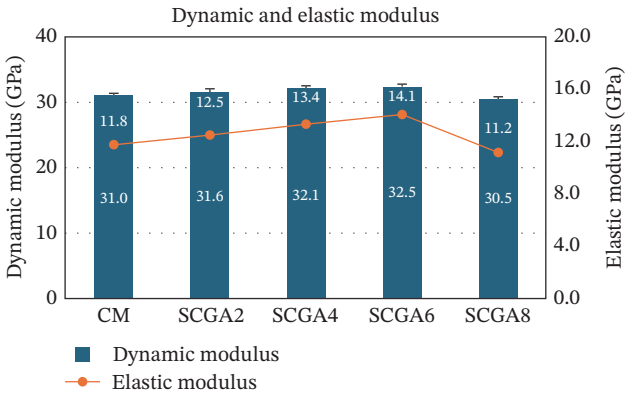



**FIGURE 5** | Dynamic and elastic moduli of modified asphalt mixtures.

### 5.1.8 | Sustainability Aspect

A simplified binder production-stage $CO_2$ comparison was carried out to assess the sustainability aspect. For a 1 tonne asphalt mixture with a binder content of 6.4%, the utilization of SCGA6 reduces the quantity of the virgin binder from 64 to 61.16 kg. The approximate emission of $CO_2$ per tonne of bitumen is assumed to be 400 kg of $CO_2$ [44]. Depending on the life cycle parameters and data source, the $CO_2$ emissions associated with the manufacture of one tonne of bitumen are often reported to range from 200 to 637 kg $CO_2$-equivalent per tonne [44]. Therefore, in this study, an average emission value of 400 kg of $CO_2$ per tonne of asphalt is adopted. With the reduced requirement of the virgin binder, the emissions decreased to 24.06 kg $CO_2$ from 25.6 kg $CO_2$ per tonne of bitumen. Although this reduction per tonne is modest, it becomes meaningful at the network scale and is achieved through partial use of bitumen with waste-derived material. A thorough sustainability evaluation requires a full life cycle assessment that considers SCGA processing energy and long-term performance.

The experimental program incorporated triplicate testing for all mixture conditions, and statistical validation was performed to evaluate the significance and reliability of the observed trends across binder-, volumetric-, mechanical-, durability-, and modulus-related properties. One-way ANOVA conducted at the 95% confidence level confirmed that the changes in key parameters, including stability, ITS, TSR, RR, FL, DM, and EM, were statistically significant ($p<0.05$), particularly when the CM was compared with the SCGA6 and SCGA8. Binder properties such as penetration, softening point, viscosity, and storage stability exhibited consistent monotonic trends with relatively low variability, indicating that the SCGA content exerted a systematic influence on binder rheology rather than random experimental fluctuations (Table 9). Similarly, the mix design parameters (Gmb, VMA, and VFA) were significantly different because of the increased binder absorption and altered aggregate packing due to the porous nature of SCGA. Mechanical performance results demonstrated that ITS dry and stability improvements up to 6% SCGA were statistically reliable, with narrow confidence intervals confirming the repeatability among the replicate samples. In contrast, the TSR values significantly decreased at 8% SCGA, validating the observed decrease to 83.6% as a true material response linked to moisture susceptibility rather than

**TABLE 9** | Statistical validation summary of SCGA-modified asphalt mixture properties.

| | Parameter | | | | | |
|---|---|---|---|---|---|---|
| **Category** | **1** | ***p*-Value** | **2** | ***p*-Value** | **3** | ***p*-Value** |
| Binder properties | Penetration | <0.05 | Softening point | <0.01 | Ductility | < 0.05 |
| | Viscosity | <0.01 | — | — | — | — |
| Volumetric properties | Gmb | <0.05 | VMA/ VFA | <0.05 | — | — |
| Mechanical properties | Stability | <0.01 | ITS dry | <0.01 | ITS wet | < 0.05 |
| | TSR | <0.01 | — | — | — | — |
| Durability & deformation | Rapid rutting (RR) | <0.05 | Fatigue life | <0.05 | — | — |
| Modulus properties | Dynamic modulus (DM) | <0.05 | Elastic modulus (EM) | <0.05 | — | — |

measurement scatter. Rutting resistance and modulus-related parameters also significantly varied, with the ANOVA results supporting the improvement trend up to the optimum dosage, followed by a performance reduction at higher SCGA contents. The FL significantly increased at moderate dosages, reflecting an improved stress distribution within the asphalt matrix. The variability observed across properties is primarily attributed to controlled differences in the air void content ($7.0 \pm 0.1\%$), binder film thickness, aggregate orientation, and heterogeneous microstructure of the biomass ash particles. Despite these influences, the relatively low standard deviations reported in the statistical summary confirm good experimental repeatability. Overall, the results of the statistical analysis validate that the performance trends reported for SCGA-modified mixtures are significant and reproducible, supporting the reliability of the experimental conclusions.

## 5.2 | Machine Learning

### 5.2.1 | Statistical Summary

A statistical summary (Table 10) of the experimental data provides a clear understanding of the effects of the BC and SCGA on the performance characteristics of asphalt mixtures. The BC used in the study ranged from 5.0% to 6.5%, with an average of 5.78%, while the SCGA replacement varied widely from 0% to 8%, with an average of 4%. The stability values, representing the load-bearing capacity of the mix, averaged 11.30 kN, with most results ranging from 10.78 to 11.80 kN, indicating a strong structural performance. The ITS under dry conditions (ITSD) averaged 678.26 kPa, whereas under wet conditions (ITSW), it decreased to 605.36 kPa, reflecting the expected effect of moisture. The TSR averaged 89.46%, significantly exceeding the minimum requirement of 80%, confirming the excellent resistance of the mixture to moisture damage and overall durability. The resilient modulus (RR) had an average value of 665 kPa, indicating that the strong recovery capacity of the mixture occurred under repeated loading. The FL, which reflects the number of load cycles to failure, averaged 14,246 cycles, demonstrating the excellent endurance of mixes modified with SCGA. The DM, which is associated with rutting resistance under stress, remained steady at ~31.33 mm, indicating minimal variation and consistent performance. The average EM was 12.53, indicating a balanced stiffness that ensures adequate flexibility to resist cracking while maintaining sufficient strength against rutting. Overall, the findings show that asphalt mixtures containing 5%–6% bitumen and up to 8% SCGA exhibit high strength, high durability, and superior resistance to moisture-related damage, confirming that SCGA is a promising sustainable additive for improving asphalt pavement performance.

**TABLE 10** | Descriptive statistical summary of input features and output variables used in machine learning models.

| **Parameters** | **Count** | **Mean** | **Std** | **Min** | **25%** | **50%** | **75%** | **Max** |
|---|---|---|---|---|---|---|---|---|
| BC | 120 | 5.78 | 0.49 | 5.00 | 5.40 | 5.90 | 6.10 | 6.5 |
| SC | 120 | 4.82 | 2.84 | 0.00 | 2.00 | 4.00 | 6.0 | 8.0 |
| ST | 120 | 11.30 | 0.63 | 9.50 | 10.78 | 11.25 | 11.80 | 12.5 |
| ITSD | 120 | 678.26 | 21.37 | 630.00 | 665.00 | 673.65 | 694.52 | 720.0 |
| ITSW | 120 | 605.36 | 30.07 | 540.00 | 580.00 | 609.80 | 631.92 | 645.0 |
| TSR | 120 | 89.46 | 2.59 | 83.58 | 88.95 | 90.25 | 91.35 | 93.1 |
| RR | 120 | 665.0 | 21.50 | 620.00 | 649.21 | 664.00 | 682.50 | 705 |
| FL | 120 | 14246.8 | 861.56 | 12100.0 | 13704.7 | 14325. | 14914.7 | 15,480 |
| DM | 120 | 31.33 | 0.85 | 29.20 | 30.58 | 31.30 | 32.12 | 32.5 |
| EM | 120 | 12.5339 | 0.97 | 11.00 | 11.73 | 12.42 | 13.42 | 14.1 |

*Note*: 25%, 50%, and 75% correspond to the first quartile (Q1), median (Q2), and third quartile (Q3), respectively.

To improve the predictive capability, robustness, and generalization performance of the developed machine learning framework, hyperparameter optimization was performed for both the decision tree and XGBoost regression models (Table 11). The optimization process was carried out using a grid-search strategy integrated with k-fold cross-validation to systematically determine the optimal combination of hyperparameters while minimizing overfitting and prediction uncertainty. The final hyperparameter configurations were selected based on the combinations that produced the highest prediction accuracy together with the lowest RMSE and MAE values on the validation dataset.

For the decision tree regression model, parameters controlling tree growth and structural complexity were optimized to improve prediction stability and prevent excessive model branching. The maximum tree depth was adjusted to avoid overfitting to the experimental dataset, whereas the minimum number of samples required for node splitting and leaf node formation was optimized to reduce sensitivity to noise within the laboratory-generated data. The optimized decision tree configuration demonstrated excellent capability in capturing the nonlinear relationships among the asphalt mixture performance parameters while maintaining low computational complexity and reduced prediction uncertainty. The optimized tree depth and splitting constraints enabled the decision tree model to effectively represent the coupled mechanical behavior of SCGA-modified asphalt mixtures without memorizing the training data. Similarly, for the XGBoost Regression model, several boosting and regularization parameters including the learning rate, maximum tree depth, number of estimators, subsampling ratio, and column sampling ratio were optimized. The learning rate controlled the contribution of each boosting iteration and improved convergence stability, while the number of estimators governed the boosting stages during model development. Subsampling and feature sampling ratios improved model generalization and reduced the dependency on specific training samples or variables. In addition, regularization parameters were incorporated to minimize excessive model complexity and improve robustness against overfitting. These optimization strategies improved prediction consistency and enabled stable model performance across different dataset partitions.

The optimized decision tree model demonstrated comparatively lower RMSE, MAE, and RSR values together with higher $R^2$ and NSE values for most of the investigated performance parameters. This behavior can be attributed to the structured nature of the experimental dataset and the strong nonlinear relationships among the mechanical properties of SCGA-modified asphalt mixtures. In comparison, the XGBoost model exhibited slightly higher prediction errors but demonstrated improved generalization capability because of the incorporation of boosting and regularization mechanisms. The regularization constraints reduced the tendency of the model to memorize training data, thereby improving its robustness and stability under unseen conditions. The integration of grid-search optimization and k-fold cross-validation significantly enhanced the reliability, robustness, and engineering applicability of the developed machine learning models. The optimized models achieved balanced predictive performance with strong accuracy, reduced overfitting sensitivity, and improved generalization capability for predicting the mechanical and durability properties of SCGA-modified asphalt mixtures. Table 10 and Figure 6 represent decision tree regression and XGBoost regression across different asphalt mixture performance parameters and actual vs predicted parameters of the decision tree and XGBboost ML models of stability, ITS dry, ITS wet, TSR, RR, FL, DM, and EM, respectively.

**TABLE 11** | Decision tree regression and XGBoost regression across different asphalt mixture performance parameters.

| Property | Model | $R^2$ | RMSE | MAE | RSR | NSE | PI | a20-index |
|---|---|---|---|---|---|---|---|---|
| Stability (kN) | Decision tree | 0.83 | 0.26 | 0.14 | 0.39 | 0.83 | 1.31 | 100 |
| | XGBoost | 0.45 | 0.48 | 0.40 | 0.73 | 0.45 | 0.83 | 100 |
| ITS dry (kPa) | Decision tree | 0.90 | 6.96 | 3.70 | 0.31 | 0.90 | 1.45 | 100 |
| | XGBoost | 0.64 | 13.23 | 9.77 | 0.59 | 0.64 | 1.03 | 100 |
| ITS wet (kPa) | Decision tree | 0.96 | 5.73 | 4.08 | 0.18 | 0.96 | 1.65 | 100 |
| | XGBoost | 0.78 | 14.39 | 12.32 | 0.46 | 0.78 | 1.21 | 100 |
| TSR (%) | Decision tree | 0.94 | 0.60 | 0.41 | 0.22 | 0.94 | 1.59 | 100 |
| | XGBoost | 0.75 | 1.32 | 1.05 | 0.48 | 0.75 | 1.17 | 100 |
| RR (kPa) | Decision tree | 0.89 | 7.17 | 4.17 | 0.31 | 0.89 | 1.44 | 100 |
| | XGBoost | 0.60 | 14.20 | 11.05 | 0.62 | 0.60 | 0.98 | 100 |
| Fatigue life | Decision tree | 0.98 | 126.29 | 75.84 | 0.13 | 0.98 | 1.73 | 100 |
| | XGBoost | 0.76 | 433.11 | 343.93 | 0.47 | 0.76 | 1.19 | 100 |
| DM | Decision tree | 0.97 | 0.12 | 0.079 | 0.14 | 0.97 | 1.73 | 100 |
| | XGBoost | 0.75 | 0.43 | 0.38 | 0.49 | 0.75 | 1.17 | 100 |
| EM | Decision tree | 0.95 | 0.21 | 0.11 | 0.20 | 0.9555 | 1.6187 | 100 |
| | XGBoost | 0.75 | 0.50 | 0.41 | 0.48 | 0.7535 | 1.1772 | 100 |

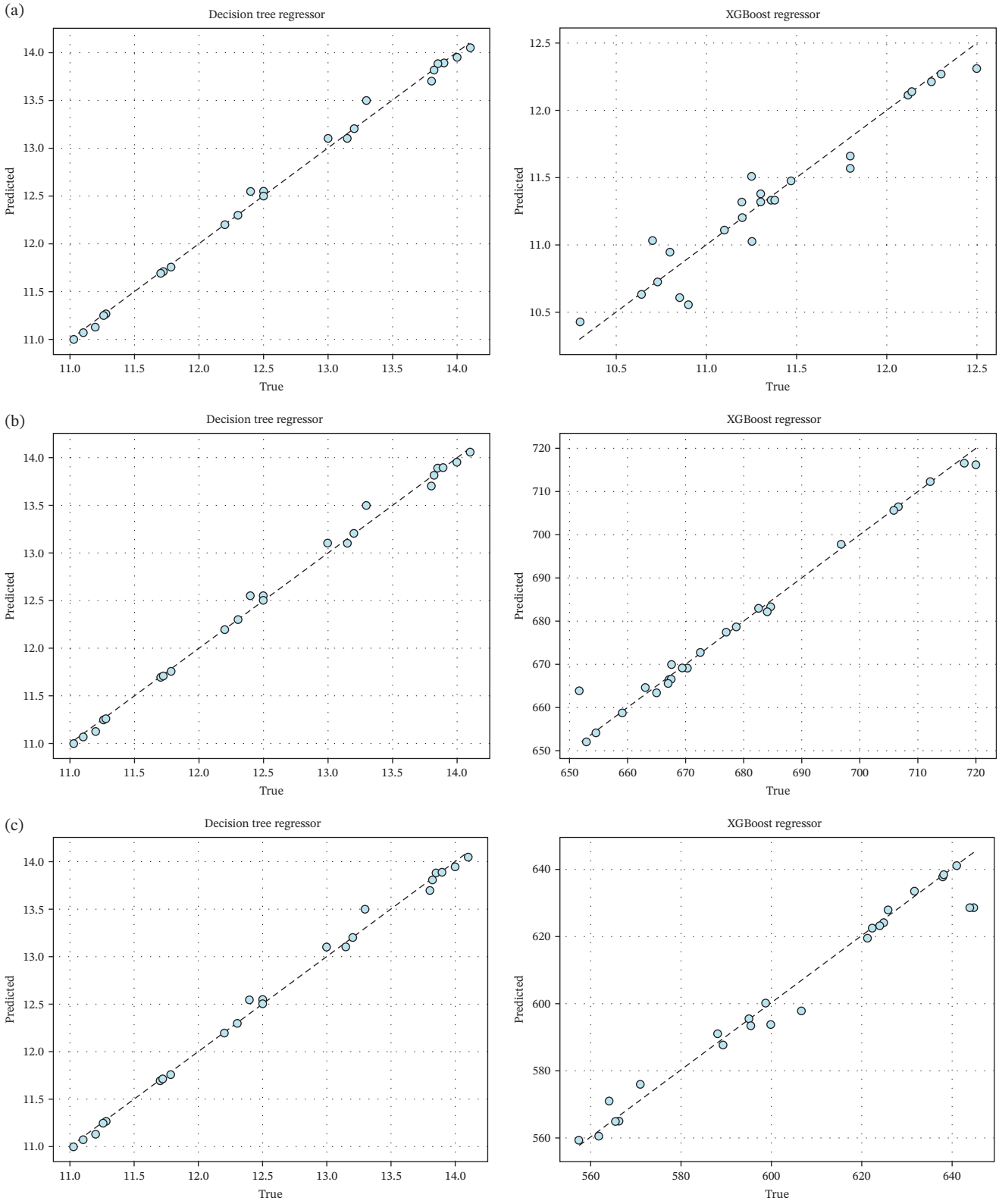



**FIGURE 6** | (Continued)

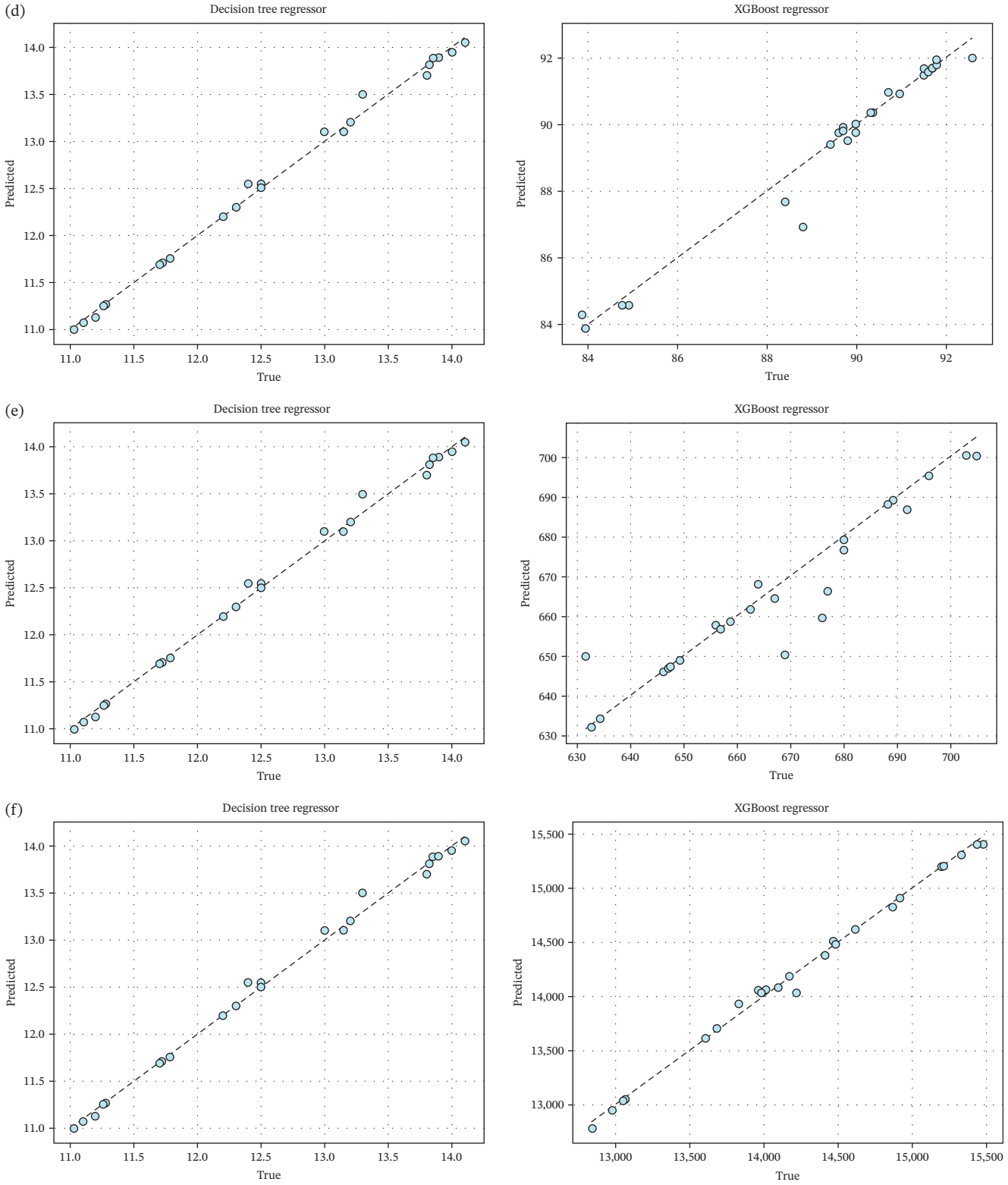



**FIGURE 6** | (Continued)

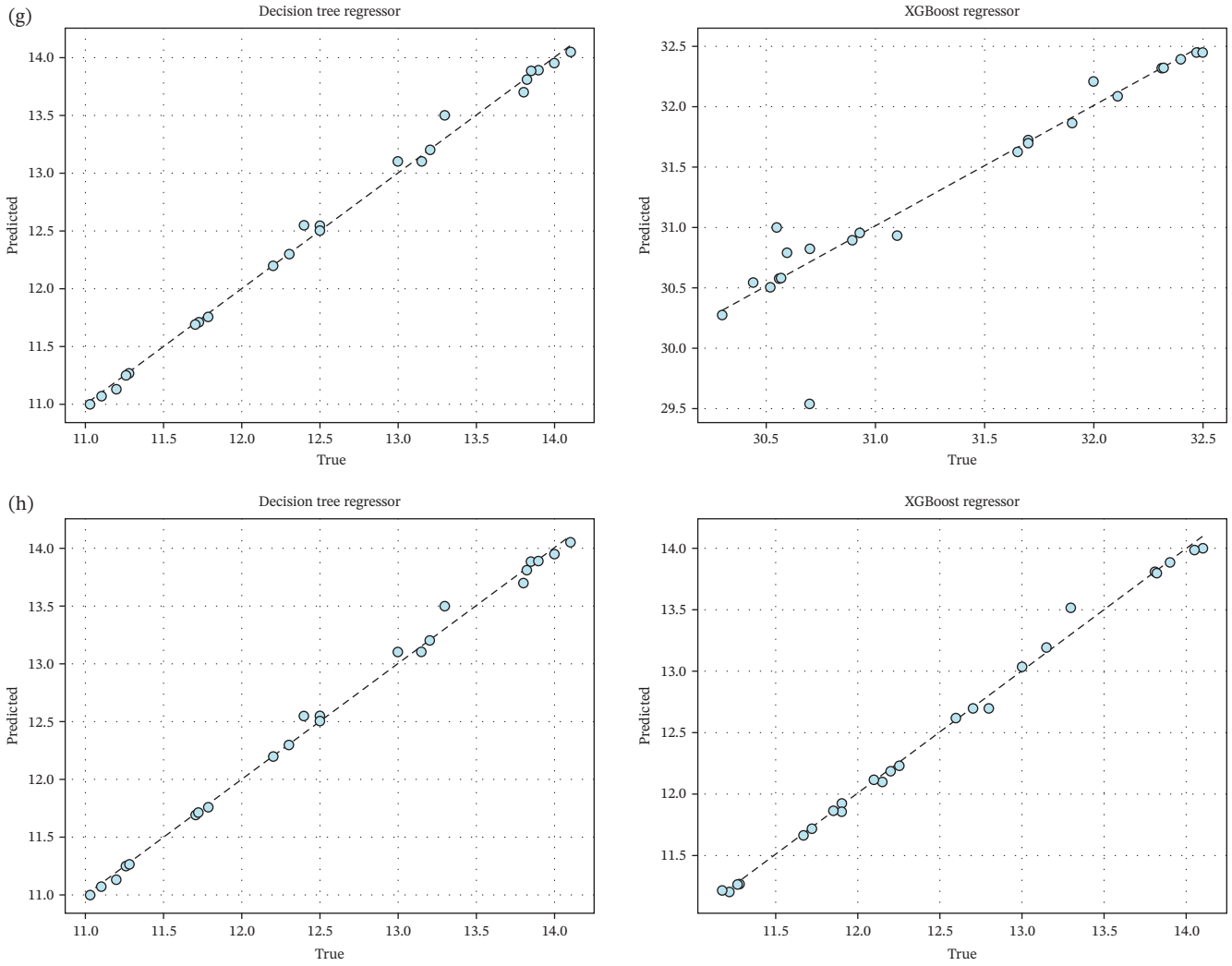



**FIGURE 6** | Actual vs predicted parameters of the decision tree and XGBboost ML models: (a) stability, (b) ITS dry (kPa), (c) ITS wet (kPa), (d) TSR (%), (e) RR (kPa), (f) fatigue life, (g) DM, (h) EM.

### 5.2.2 | k-Fold Cross-Validation Analyses

Figure 7 presents the comparative convergence behavior of the decision tree and XGBoost models obtained through k-fold cross-validation analysis. The plots illustrate the variation of MSE with increasing k-fold values ranging from 1 to 45. The purpose of this analysis was to evaluate the prediction stability, convergence characteristics, and robustness of the developed machine learning models under different validation conditions. The decision Tree model demonstrated comparatively lower MSE values and faster convergence behavior across the

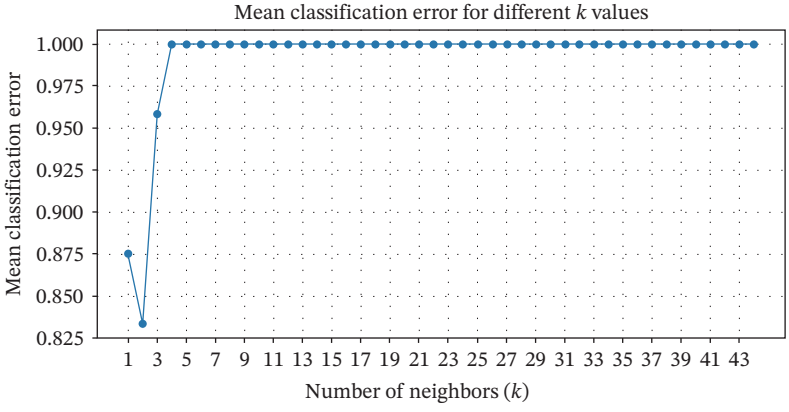



**FIGURE 7** | k-fold cross-validation analyses.

investigated fold range. The fluctuations in MSE values gradually reduced with increasing fold numbers, indicating stable predictive performance and reduced sensitivity to dataset partitioning. The lower convergence error observed for the decision Tree model confirms its strong capability to capture the nonlinear relationships governing the mechanical properties of SCGA-modified asphalt mixtures. In comparison, the XGBoost model exhibited relatively higher MSE values during the initial folds; however, the convergence trend became smoother and more stable at higher fold numbers because of the boosting and regularization mechanisms incorporated within the model. Although the XGBoost model demonstrated slightly higher prediction errors compared with the Decision Tree model, the reduced fluctuation in convergence behavior indicates improved generalization capability and resistance to overfitting. The stabilization of MSE values at higher k-fold numbers confirms the robustness and consistency of the developed machine learning framework. The comparative k-fold convergence analysis demonstrates that both models achieved stable predictive performance, whereas the Decision Tree model exhibited comparatively superior convergence accuracy and lower prediction uncertainty for the investigated asphalt mixture performance parameters.

### 5.2.3 | SHAP Analysis

SHAP analysis (Figure 8) was employed to quantify the relative contribution of the input variables to predicting the performance parameters of the asphalt mixture, including the stability (kN), ITS dry (kPa), ITS wet (kPa), TSR (%), resilient modulus (RR), FL, DM, and EM. The SHAP summary plots provide insight into both the magnitude and direction of feature influence, enabling an interpretable assessment of model behavior that complements experimental observations and established pavement engineering principles. The SHAP results consistently identify ITS and modulus-related parameters as the dominant predictors. This outcome is physically consistent with the experimental findings, where the dry temperature of ITS increased from 650 kPa in the CM to 720 kPa in SCGA6, accompanied by an increase in FL from 13,800 to 15,480 cycles. Similarly, the stiffness-related properties strongly influence the material, with an average DM of 31.33 GPa and an EM of 14.1 GPa at the optimum SCGA dosage. These trends indicate that the predictive models primarily respond to parameters governing tensile resistance and stiffness, which are fundamental to stress transfer, load distribution, and structural stability under repeated traffic loading. From a mechanistic standpoint, the ITS reflects the resistance of the mixture to tensile stresses generated by traffic and environmental actions, whereas the modulus parameters control the deformation characteristics and rutting resistance. The SHAP distributions demonstrate that higher ITS values shift predictions toward improved stability and fatigue performance, which is consistent with the observed increase in stability from 10.5 to 12.5 kN at SCGA6 (≈19% improvement). However, the analysis also reveals diminishing returns at excessive stiffness levels. At 8% SCGA, the TSR decreased from 93.1% to 83.6%, and the FL decreased to 12,950 cycles, highlighting the trade-off between stiffness enhancement and durability. Similarly, the RR increased from 630 to 705 kPa at SCGA6, confirming the improved load-bearing capacity but also indicating the sensitivity of the mixture performance to excessive stiffening. The comparatively lower SHAP importance assigned to the SCGA dosage does not imply a lack of engineering relevance; rather, it reflects the indirect role of SCGA in modifying key mechanical properties such as tensile strength and stiffness. Although the SCGA content ranged from 0% to 8%, its influence became prominent primarily through its effect on the ITS and modulus values, which explains the apparent discrepancy between the experimental significance and direct SHAP ranking. This observation highlights the interconnected nature of asphalt mixture performance, where the additive dosage influences behavior through secondary mechanical responses rather than acting as an independent governing variable. From a mixture design perspective, the SHAP analysis provides practical insights for performance-based optimization. The dominance of the ITS and modulus underscores the necessity of maintaining a balanced stiffness–flexibility relationship when the SCGA dosage is selected. Numerical trends indicate that SCGA6 achieves this balance, with an ITS dry of 720 kPa, an RR of 705 kPa, and a FL of 15,480 cycles, whereas further increases in SCGA content reduce moisture resistance and long-term durability. The agreement between the SHAP rankings and established pavement mechanics confirms the physical plausibility of the predictive framework and reinforces its applicability as a decision-support tool for sustainable asphalt mixture design. It should be emphasized that SHAP analysis quantifies the influence of statistical features within the predictive model rather than establishing causal relationships between variables. The reported feature importance values therefore represent contributions to model predictions and must be interpreted alongside experimental evidence and fundamental engineering understanding. Overall, the explainable AI framework enhances the interpretability of machine learning predictions while maintaining consistency with observed material behavior.

**5.2.3.1 | Cosine Amplitude Sensitivity Analysis (CASA).** The CASA was performed to evaluate the relative influence of the input variables on the prediction of asphalt mixture performance parameters. CASA quantifies the degree of association between input and output variables by measuring the cosine angle between feature vectors. Higher cosine amplitude values indicate a stronger influence and greater sensitivity of the input parameter toward the corresponding output variable.

The cosine amplitude relationship is expressed as:

$$r_{ij} = \frac{\sum_{k=1}^{n} x_{ik} y_{jk}}{\sqrt{\sum_{k=1}^{n} x_{ik}^2} \sqrt{\sum_{k=1}^{n} y_{jk}^2}},$$

where $r_{ij}$ represents the sensitivity coefficient between the input and output variables, $x_i$ denotes the input feature vector, and $y_j$ represents the output parameter vector.

CASA was performed to quantify the influence of the input variables on the predicted mechanical and durability properties of SCGA-modified asphalt mixtures. The CASA technique evaluates the strength of association between the input and output variables by measuring the cosine similarity between their corresponding vectors. Higher CASA values indicate stronger sensitivity and a greater influence of a particular feature on the predicted output parameter.

The results presented in Table 12 indicate that BC exhibited the highest sensitivity toward all predicted performance parameters,

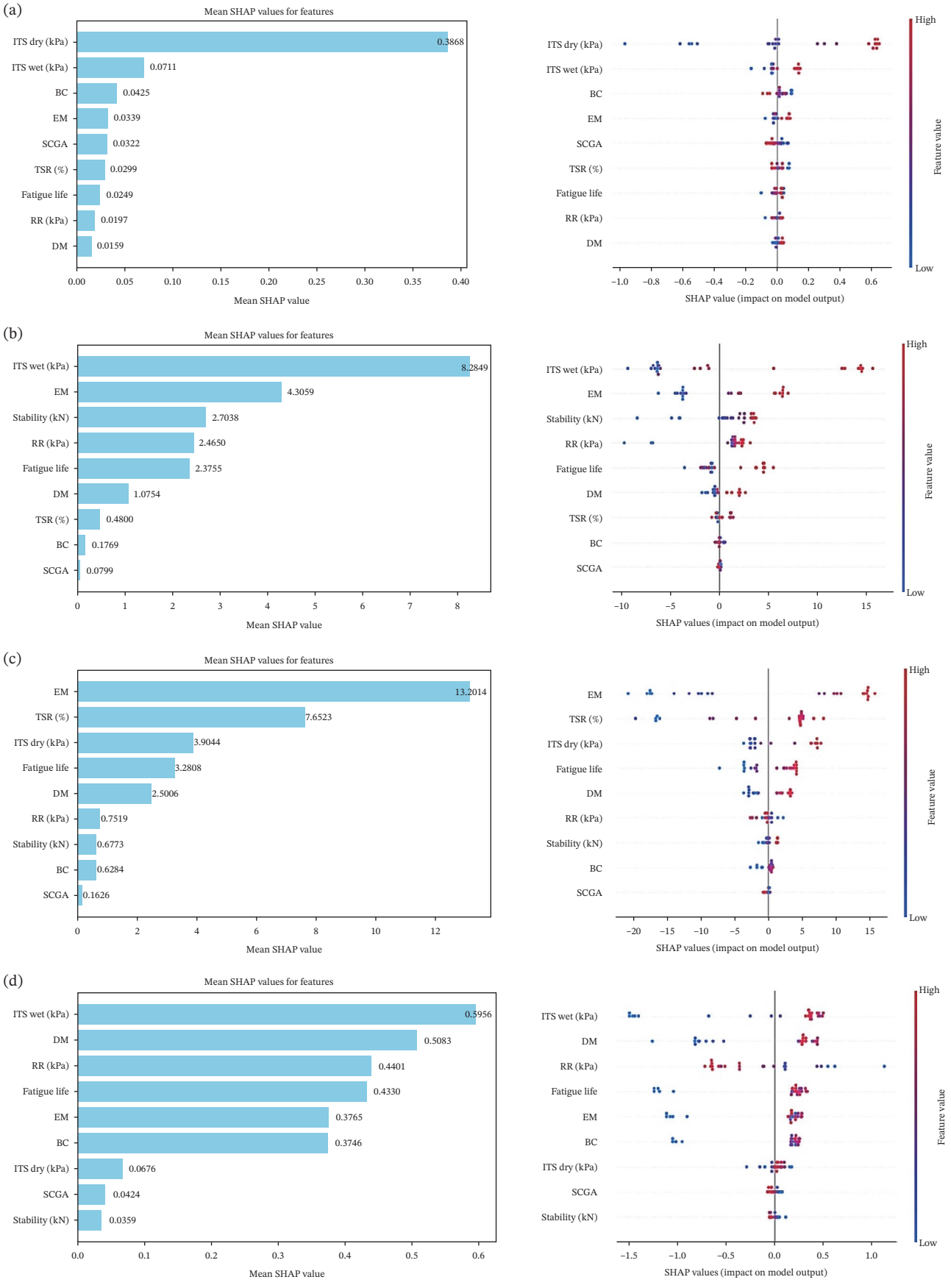



**FIGURE 8** | (Continued)

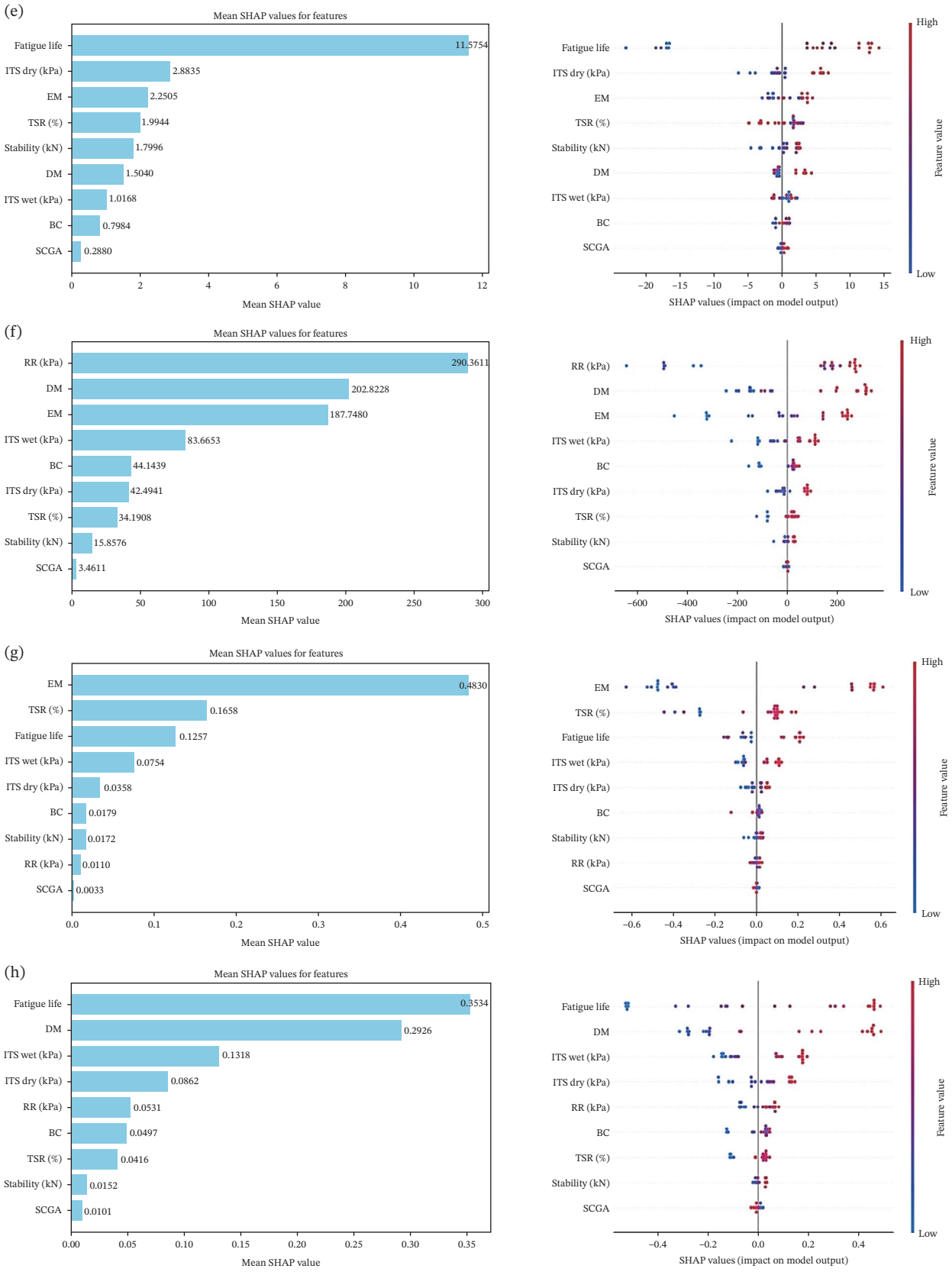



**FIGURE 8** | SHapley Additive exPlanations (SHAP) analysis: (a) Stability, (b) ITS dry (kPa), (c) ITS wet (kPa), (d) TSR (%), (e) RR (kPa), (f) fatigue life, (g) DM, (h) EM.

**TABLE 12** | Cosine amplitude sensitivity analysis results.

| Input feature | Output parameter | CASA value | Input feature | Output parameter | CASA value |
|---|---|---|---|---|---|
| BC | Stability (kN) | 0.99 | SCGA | Stability (kN) | 0.86 |
| BC | ITS dry (kPa) | 0.99 | SCGA | ITS dry (kPa) | 0.86 |
| BC | ITS wet (kPa) | 0.99 | SCGA | ITS wet (kPa) | 0.85 |
| BC | TSR (%) | 0.99 | SCGA | TSR (%) | 0.85 |
| BC | RR (kPa) | 0.99 | SCGA | RR (kPa) | 0.86 |
| BC | Fatigue life | 0.99 | SCGA | Fatigue life | 0.86 |
| BC | DM | 0.99 | SCGA | DM | 0.86 |
| BC | EM | 0.99 | SCGA | EM | 0.86 |

with CASA values ranging from 0.9944 to 0.9973. These very high sensitivity values demonstrate that the BC plays a dominant role in controlling the mechanical and durability behavior of asphalt mixtures. Among all the output parameters, the TSR and FL exhibited particularly high sensitivity toward BC, with CASA values of 0.9973 and 0.9970, respectively. This behavior indicates that the binder content strongly influences moisture resistance, stiffness characteristics, fatigue resistance, and long-term durability of asphalt mixtures.

Similarly, resilient modulus (RR), ITS, DM, and EM also demonstrated very high sensitivity toward BC. These results confirm that variations in binder content significantly affect the stiffness, elasticity, deformation resistance, and cracking behavior of asphalt mixtures. The strong relationship observed between BC and the modulus-related parameters further validates the experimental findings, where changes in binder content directly influenced the internal bonding characteristics and load-transfer mechanisms within the asphalt matrix.

The SCGA dosage also demonstrated considerable influence on the predicted performance parameters, with CASA values ranging between 0.8593 and 0.8660. Although these sensitivity values were lower than those of BC, they still indicate a strong interaction between SCGA incorporation and asphalt mixture performance. Among the investigated parameters, resilient modulus (RR) and FL exhibited comparatively higher sensitivity toward SCGA dosage, indicating that SCGA primarily influences stiffness enhancement and long-term deformation resistance characteristics of asphalt mixtures.

The comparatively lower CASA values associated with SCGA dosage suggest that its influence is more indirect and depends on its interaction with the binder and aggregate matrix. The porous and angular morphology of SCGA particles improves binder absorption and internal friction, thereby enhancing the stiffness and rutting resistance. However, excessive SCGA incorporation may reduce the effective binder film thickness and increase brittleness, which affects moisture resistance and fatigue performance. This behavior is consistent with the experimental observations obtained from ITS, TSR, and FL tests.

The CASA results confirm that both BC and SCGA dosage significantly influence the mechanical and durability properties of asphalt mixtures, with the BC acting as the most dominant governing parameter. The sensitivity analysis further validates the reliability of the developed machine learning framework and improves interpretability by identifying the most influential variables governing asphalt mixture performance.

#### 5.2.4 | REC Curve and Taylor Diagram Analysis

An analysis of the REC curve and Taylor diagram (Figure 9) clearly demonstrates the superior performance of the XGBoost regressor across most parameters compared with the decision tree model. The REC curves for stability, ITS dry, ITS wet, TSR, FL, DM, and EM show that the XGBoost predictions are closely aligned with the experimental values, as most data points lie near the diagonal line with minimal deviation, reflecting very low error rates. This is particularly evident in the ITS dry, TSR, and FL, where the curve sharply increases and reaches high accuracy thresholds, confirming the robustness of the model. In contrast, the REC curves for RR and DM show relatively wider error margins with a slower increase, indicating weaker prediction accuracy than for the other properties. The Taylor diagram further supports these observations by providing a holistic view of correlation, standard deviation, and RMSE. For most of the evaluated properties, the XGBoost predictions are closely aligned with the observed reference data, with high correlation coefficients ($R^2 > 0.9$) and minimal error values. This finding demonstrates the strong ability of the model to accurately reflect the variability present in the experimental results. However, the RR and DM predictions are positioned slightly farther from the reference point in the Taylor diagram, indicating a relatively low correlation and high deviation. On the other hand, the decision tree regressor unrealistically plots at the reference point with perfect correlation and zero error across all properties, which strongly suggests overfitting or evaluation on training data rather than a true test set. The REC curve and Taylor diagram together confirm that the XGBoost Regressor is a reliable and generalizable model for predicting stability, ITS, TSR, FL, and EM with very high accuracy, whereas RR and DM require further model refinement or feature improvement to achieve similar performance.

Although the decision tree model achieved very high $R^2$ values and extremely low error metrics, its near-perfect alignment with reference data suggests that the model may capture dataset-specific patterns more strongly than generalized relationships. Decision trees are inherently prone to overfitting when trained on relatively structured laboratory datasets with limited variability. Therefore, pruning constraints and k-fold cross-validation were employed to mitigate this effect; however, caution is needed

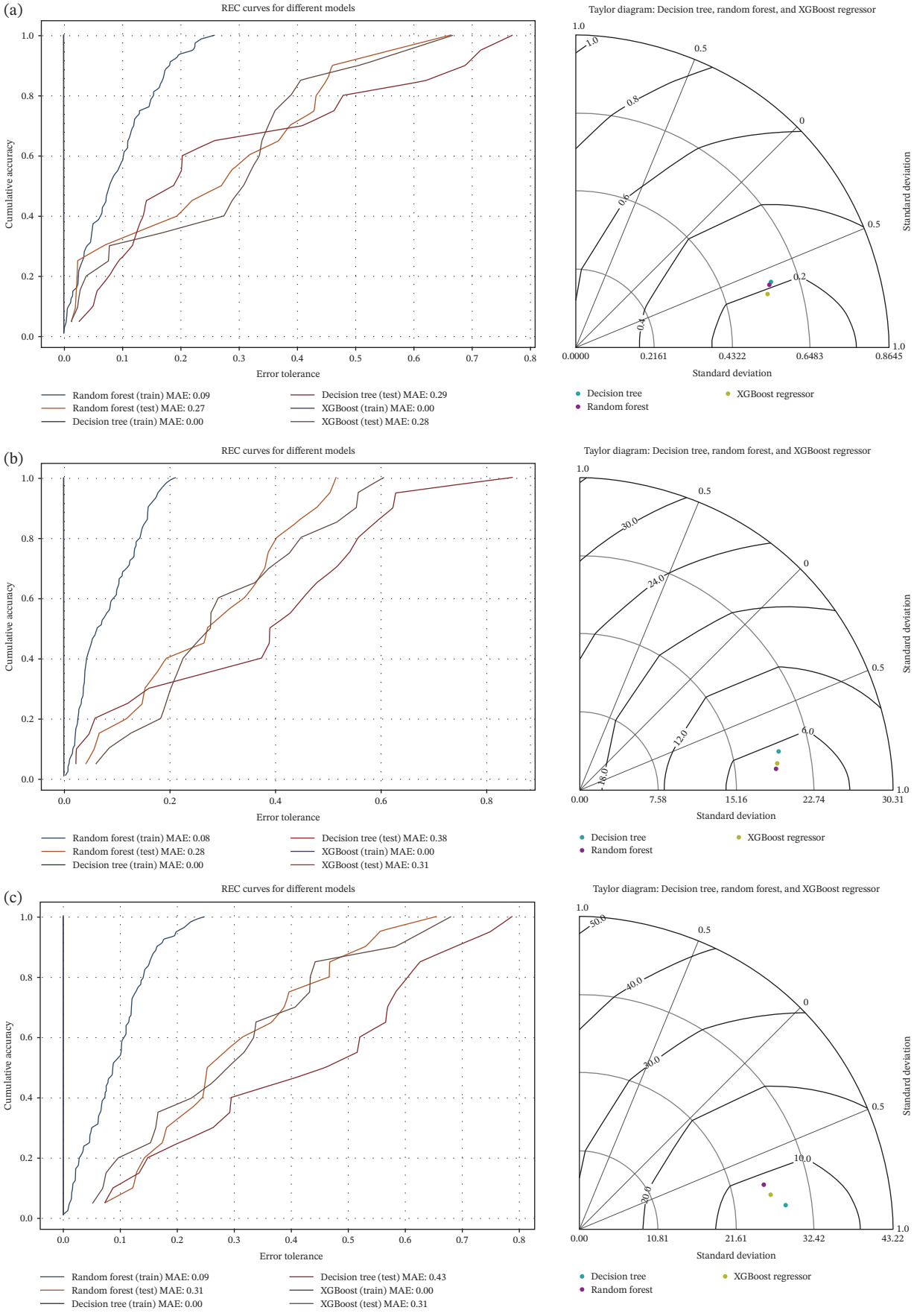
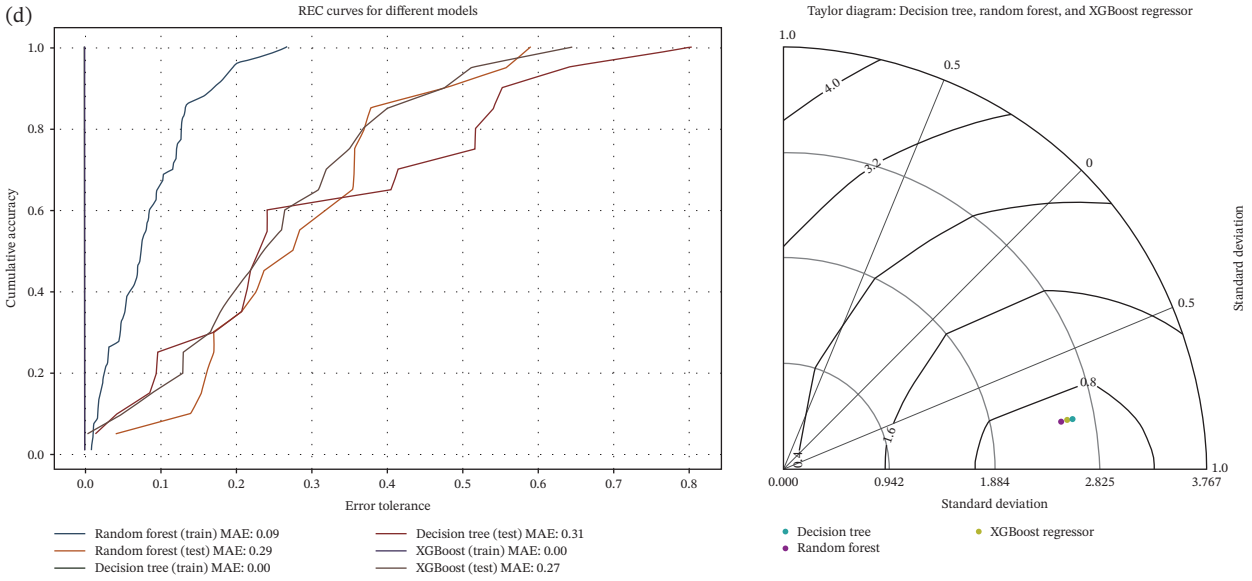
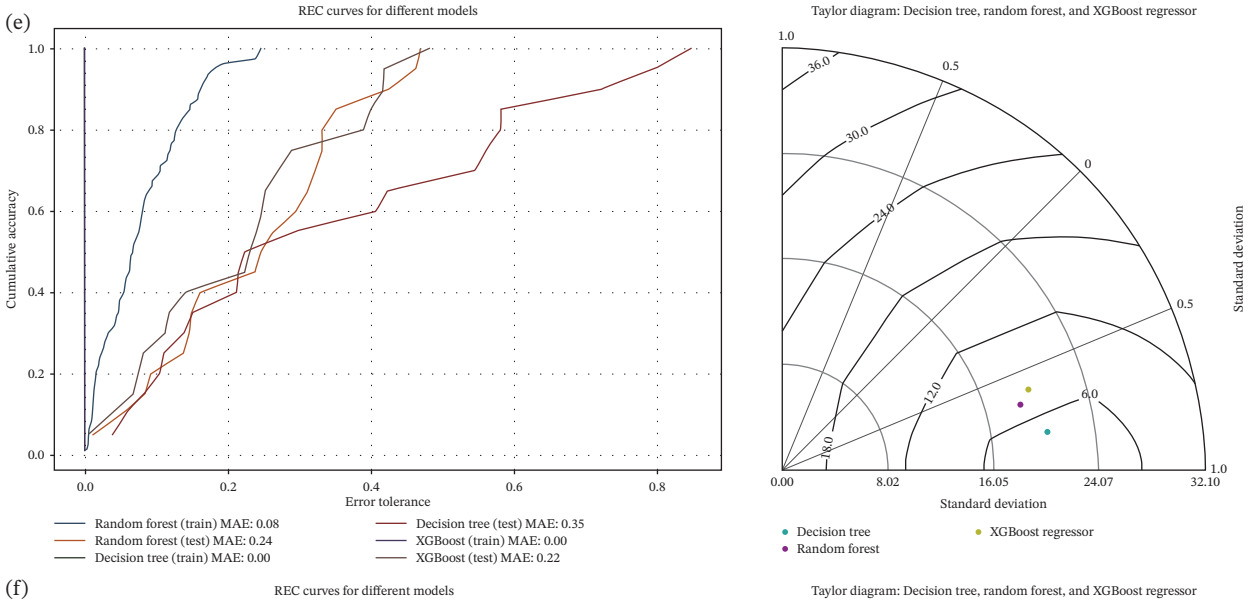



**FIGURE 9** | (Continued)



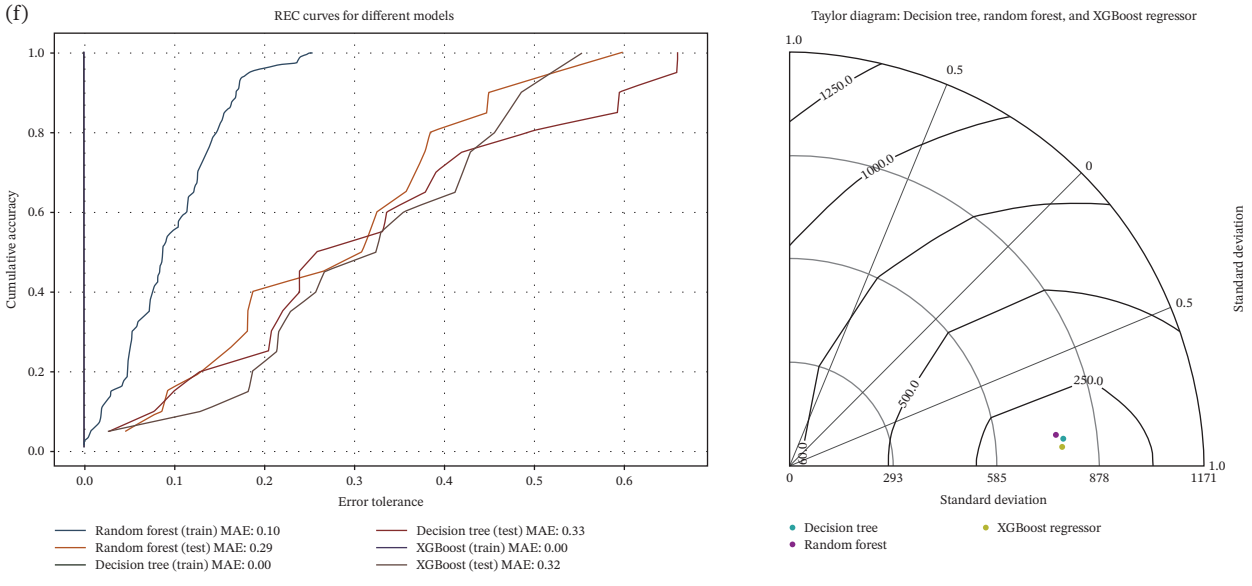




**FIGURE 9** | (Continued)

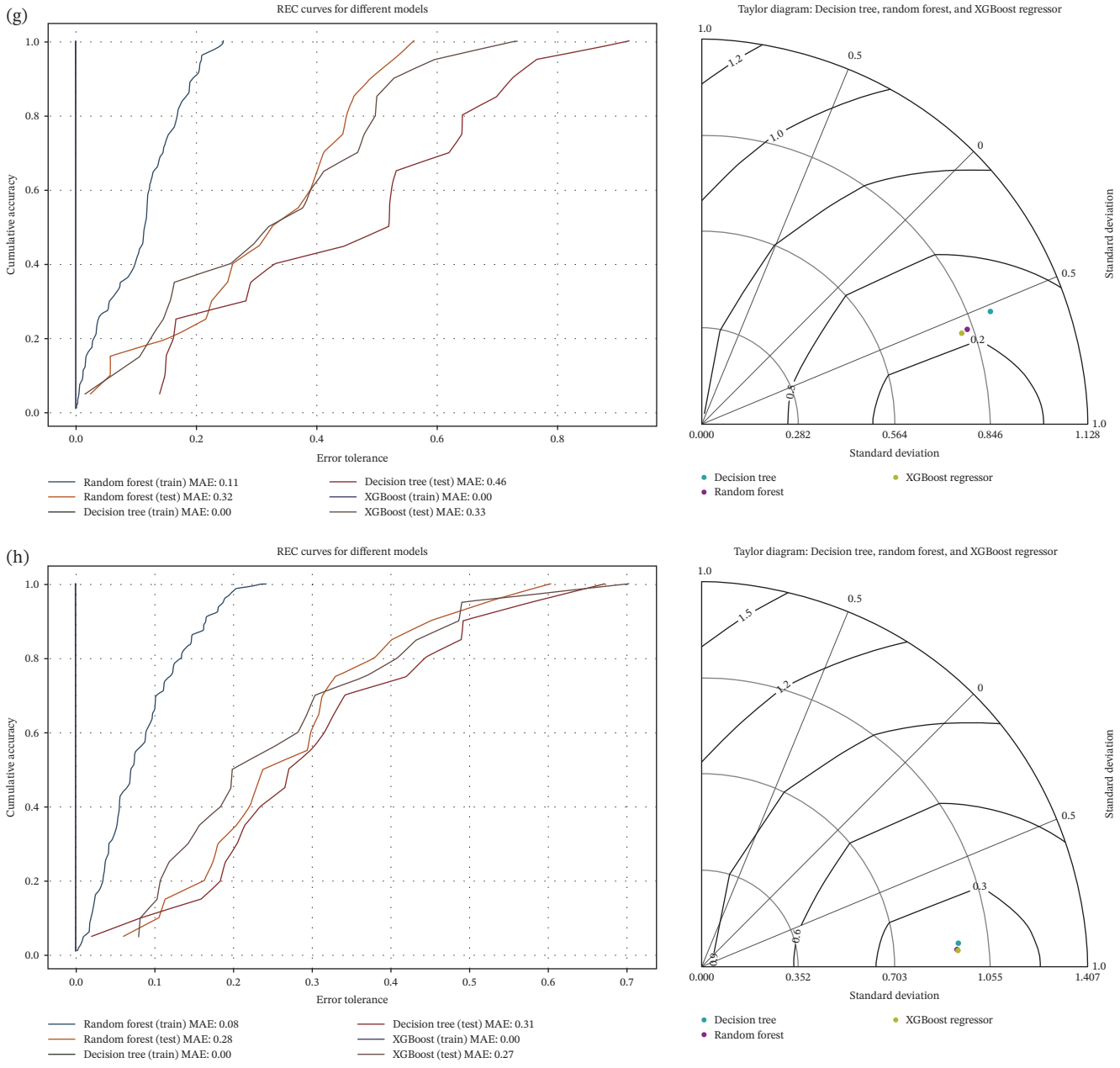



**FIGURE 9** | REC curve and Taylor diagram of various parameters: (a) Stability, (b) ITS dry (kPa), (c) ITS wet (kPa), (d) TSR (%), (e) RR (kPa), (f) fatigue life, (g) DM, (h) EM.

when extrapolating predictions beyond the investigated SCGA dosage range or outside controlled laboratory conditions. The XGBoost model, which incorporates regularization and ensemble learning, demonstrated slightly lower accuracy but stronger generalization behavior, indicating its higher reliability for broader engineering applications.

## 6 | Conclusions

An experimental and computational investigation of SCGA as a biomodifier for asphalt binders and mixtures yielded the following key conclusions across parameters:

- Incorporation of SCGA increased the stiffness and high-temperature performance of the binder, as evidenced by the reduction in penetration (66–52 mm – SCGA8), increase in softening point (49–55.3°C), and increase in viscosity (355–530 mPa·s). However, the reduction in ductility (130–70 cm) and flash point (330–260°C) indicates reduced flexibility and thermal stability at higher SCGA contents.
- The viscosity increased significantly from 355 mPa·s (CB) to 530 mPa·s (SCGA8), indicating increased stiffness. The storage stability improved from 0.3 to 1.6°C, minimizing phase separation and improving binder reliability during storage and transportation.
- Marshall mix design results demonstrated that SCGA modification improved mixture stability from 10.5 to 12.5 kN at 6% SCGA while slightly reducing bulk density due to the low specific gravity of SCGA. The increase in VMA and

VFA indicates improved binder accommodation within the asphalt matrix.

- Moisture susceptibility and fatigue performance improved up to 6% SCGA content. The ITS dry strength increased from 650 to 720 kPa, and the FL improved from 13,800 to 15,480 loading cycles. However, excessive SCGA addition (8%) reduced the TSR and fatigue resistance due to excessive stiffening of the mixture.
- Compared with the control, SCGA6 enhanced the modulus values by ~5%, but further addition (SCGA8) reduced the stiffness and recovery capacity.
- The decision tree model achieved very high predictive accuracy ($R^2$ up to 0.98); however, its near-perfect performance indicates potential sensitivity to laboratory-specific patterns. K-fold validation and pruning were therefore applied to improve the robustness. In comparison, XGBoost showed slightly lower accuracy but stronger generalization capability, suggesting higher reliability for real-world applications.

SCGA can be used as a biomodifier for asphalt binders, and an optimum dosage of 6% is recommended on the basis of stability and strength properties, fatigue, rutting, and moisture resistance without compromising durability. In this study, the reporting of 6% SCGA as the optimal dosage is based on laboratory-scale performance indicators. Although this dosage demonstrates a favorable stiffness–durability balance under controlled conditions, the field performance and long-term aging behavior should be assessed in future work.

Although the developed ML framework demonstrates strong predictive ability, the relatively limited dataset size (120 samples) may restrict extrapolation beyond the investigated material range, and future studies should incorporate larger multisource datasets to enhance generalizability.

## 7 | Limitations

Although the decision tree and XGBoost models demonstrated high predictive accuracy, the training dataset was generated using a single aggregate source and a VG-30 binder grade, which may limit model transferability to mixtures with different aggregate mineralogies, gradations, or binder chemistries. Variations in surface texture, binder–filler interactions, and moisture sensitivity can influence stiffness and durability responses, potentially affecting prediction reliability outside the investigated conditions. Therefore, the current models should be interpreted as material-specific predictive tools rather than universally generalizable frameworks. Future research should incorporate external datasets and multisource material combinations to increase robustness and enable broader applications in pavement engineering practice.

**Funding**

This work did not receive any funding.

**Conflicts of Interest**

The authors declare no conflicts of interest.

**Data Availability Statement**

Data can be made available upon request by interested parties.

**References**

1. G. S. Kumar, M. S. Ujwal, H. A. Kumar, Y. H. Sudeep, and G. Venkatesha, "Evaluating the Impact of Spent Coffee Grounds on Concrete's Workability and Mechanical Properties Using Response Surface Methodology," *Innovative Infrastructure Solutions* 10, no. 2 (2025): 70.

2. J. Huang, G. S. Kumar, and Y. Sun, "Evaluation of Workability and Mechanical Properties of Asphalt Binder and Mixture Modified With Waste Toner," *Construction and Building Materials* 276 (2021): 122230.

3. X. Zou, H. Xie, J. Li, et al., "Innovative Application of Coffee Grounds Oil as an Asphalt Modifier: Extraction, Preparation, and Rheological Properties," *Case Studies in Construction Materials* 21 (2024): e04012.

4. M. Arabani and Z. M. Moghaddam, "A Comparative Study Into the Effect of Spent Coffee Powder and Ash on Improving the Mechanical Properties of Bitumen," *Construction and Building Materials* 449 (2024): 138319.

5. S. Kalampokis, J. Valentin, E. Manthos, and A. A. Konstantinidis, "Investigation of the Rheological Properties and Ageing Susceptibility of Bitumen Bio-Modified With Spent Coffee Grounds," *Construction Materials* 5, no. 3 (2025): 45.

6. Q. Lu, A. Sha, W. Jiao, et al., "Waste Coffee Biochar and Bi-Oil Composite Modified Rejuvenated Asphalt: Preparation, Characterization, and Performance Evaluation," *Construction and Building Materials* 450 (2024): 138588.

7. N. Saboo, M. Sukhija, D. Mehta, K. Haswanth, A. Srivastava, and A. Patil, "Use of Raw Sugarcane Molasses as a Partial Replacement of Asphalt Binder: An Experimental Investigation," *Construction and Building Materials* 369 (2023): 130541.

8. C. Vargas and A. E. Hanandeh, "Features Importance and Their Impacts on the Properties of Asphalt Mixture Modified With Plastic Waste: A Machine Learning Modeling Approach," *International Journal of Pavement Research and Technology* 16, no. 6 (2023): 1555–1582.

9. F. Giustozzi, "Polymer-Modified Pervious Concrete for Durable and Sustainable Transportation Infrastructures," *Construction and Building Materials* 111 (2016): 502–512.

10. J. Huang, G. S. Kumar, J. Ren, Y. Sun, Y. Li, and C. Wang, "Towards the Potential Usage of Eggshell Powder as Bio-Modifier for Asphalt Binder and Mixture: Workability and Mechanical Properties," *International Journal of Pavement Engineering* 23, no. 10 (2022): 3553–3565.

11. G. Shiva Kumar and A. U. Ravi Shankar, "Evaluation of Workability and Mechanical Properties of Stone Matrix Asphalt Mixtures Made With and Without Stabilizing Additives," *Transportation Infrastructure Geotechnology* 7, no. 2 (2020): 191–204.

12. A. D. Stakston, H. U. Bahia, and J. J. Bushek, "Effect of Fine Aggregate Angularity on Compaction and Shearing Resistance of Asphalt Mixtures," *Transportation Research Record: Journal of the Transportation Research Board* 1789, no. 1 (2002): 14–24.

13. X. C. Schmidt Rivera, A. Gallego-Schmid, V. Najdanovic-Visak, and A. Azapagic, "Life Cycle Environmental Sustainability of Valorisation Routes for Spent Coffee Grounds: From Waste to Resources," *Resources, Conservation and Recycling* 157 (2020): 104751.

14. U. Rongali, G. Singh, A. Chourasiya, and P. K. Jain, "Laboratory Investigation on Use of Fly Ash Plastic Waste Composite in Bituminous Concrete Mixtures," *Procedia - Social and Behavioral Sciences* 104 (2013): 89–98.

15. P. J. Bosscher, H. U. Bahia, S. Thomas, and J. S. Russell, "Relationship Between Pavement Temperature and Weather Data: Wisconsin Field Study to Verify Superpave Algorithm," *Transportation Research Record: Journal of the Transportation Research Board* 1609, no. 1 (1998): 1–11.

16. C. Hu, J. Zhao, Z. Leng, M. N. Partl, and R. Li, "Laboratory Evaluation of Waterborne Epoxy Bitumen Emulsion for Pavement Preventative Maintenance Application," *Construction and Building Materials* 197 (2019): 220–227.

17. J. Huang, X. Li, G. S. Kumar, Y. Deng, M. Gong, and N. Dong, "Rheological Properties of Bituminous Binder Modified With Recycled Waste Toner," *Journal of Cleaner Production* 317 (2021): 128415.

18. M. Y. Fattah, M. M. Hilal, and H. B. Flyeh, "Evaluation of the Mechanical Stability of Asphalt Mixture Using the Gyratory Compactor," *International Journal of Pavement Research and Technology* 12, no. 5 (2019): 508–518.

19. W. Fedrigo, W. P. Núñez, and A. T. Visser, "A Review of Full-Depth Reclamation of Pavements With Portland Cement: Brazil and Abroad," *Construction and Building Materials* 262 (2020): 120540.

20. K. Murari, R. Siddique, and K. K. Jain, "Use of Waste Copper Slag, a Sustainable Material," *Journal of Material Cycles and Waste Management* 17, no. 1 (2015): 13–26.

21. A. T. Tessema, N. M. Wolelaw, and G. A. Alene, "Experimental Evaluation of Coffee Husk Ash as a Filler in Hot Mix Asphalt Concrete Productions," *Advances in Civil Engineering* 2022, no. 1 (2022): 6726700.

22. L.-K. Lin, T.-M. Kuo, and Y.-S. Hsu, "The Application and Evaluation Research of Coffee Residue Ash Into Mortar," *Journal of Material Cycles and Waste Management* 18, no. 3 (2016): 541–551.

23. A. C. De Almeida, Q. C. De Abreu, S. P. Ribeiro, C. De Souza, and S. Pereira, "Evaluation of Partial Sand Replacement by Coffee Husks in Concrete Production," *Journal of Environmental Science and Engineering B* 8, no. 4 (2019): 129–133.

24. R. M. Jalkh, "Oil Extracts From Spent Coffee Grounds and Waste Cooking Oil to Modify the Physical Properties of Recycled Asphalt Binder," (2016).

25. H. A. Obaid, A. Eltwati, M. R. Hainin, M. A. Al-Jumaili, and M. Enieb, "Modeling and Design Optimization of the Performance of Stone Matrix Asphalt Mixtures Containing Low-Density Polyethylene and Waste Engine Oil Using the Response Surface Methodology," *Construction and Building Materials* 446 (2024): 138037.

26. J. K. Appiah, V. N. Berko-Boateng, and T. A. Tagbor, "Use of Waste Plastic Materials for Road Construction in Ghana," *Case Studies in Construction Materials* 6 (2017): 1–7.

27. V. P. Le, "Performance of Asphalt Binder Containing Sugarcane Waste Molasses in Hot Mix Asphalt," *Case Studies in Construction Materials* 15 (2021): e00595.

28. S. Sathvik, G. S. Kumar, A. Bahrami, et al., "Evaluation of Asphalt Binder and Mixture Properties Utilizing Fish Scale Powder as a Biomodifier," *Case Studies in Construction Materials* 20 (2024): e03238.

29. A. V. Kataware and A. Shantharam, "Review on Influence of Organic and Inorganic Phase Change Materials on Performance of Asphalt Binder and Asphalt Mix," *International Journal of Pavement Research and Technology* 2025 (2025): 554.

30. K. Kanitpong, N. Charoentham, and S. Likitlersuang, "Investigation on the Effects of Gradation and Aggregate Type to Moisture Damage of Warm Mix Asphalt Modified With Sasobit," *International Journal of Pavement Engineering* 13, no. 5 (2012): 451–458.

31. T. Chompoorat, T. Thepumong, P. Nuaklong, P. Jongvivatsakul, and S. Likitlersuang, "Alkali-Activated Controlled Low-Strength Material Utilizing High-Calcium Fly Ash and Steel Slag for Use as Pavement Materials," *Journal of Materials in Civil Engineering* 33, no. 8 (2021): 3798.

32. T. Chompoorat, T. Maikhun, and S. Likitlersuang, "Cement-Improved Lake Bed Sedimentary Soil for Road Construction," *Proceedings of the Institution of Civil Engineers - Ground Improvement* 172, no. 3 (2019): 192–201.

33. S. Likitlersuang and T. Chompoorat, "Laboratory Investigation of the Performances of Cement and Fly Ash Modified Asphalt Concrete Mixtures," *International Journal of Pavement Research and Technology* 9, no. 5 (2016): 337–344.

34. S. Anjan Kumar and A. Veeraragavan, "Performance Based Binder Type Selection Using Mixed Integer Programming Technique," *Construction and Building Materials* 24, no. 11 (2010): 2091–2100.

35. N. H. C. Gómez, M. Oeser, and O. Fleischel, "Chemical Modification of Bitumen With Novel Isocyanate-Based Additive to Enhance Asphalt Performance," *Construction and Building Materials* 301 (2021): 124128.

36. M. Sienkiewicz, M. M. Pław Gnatowski, A. Grzegórska, et al., "Eco-Friendly Modification of Bitumen: The Effects of Rubber Wastes and Castor Oil on the Microstructure, Processability and Properties," *Journal of Cleaner Production* 447 (2024): 141524.

37. N. S. A. Yaro, M. B. Napiah, M. H. Sutanto, A. Usman, and S. M. Saeed, "Modeling and Optimization of Mixing Parameters Using Response Surface Methodology and Characterization of Palm Oil Clinker Fine Modified Bitumen," *Construction and Building Materials* 298 (2021): 123849.

38. R. Mahesh, S. Kumar, and P. Pandit, "Sustainable Concrete Development Using Groundnut Shell Ash: A Response Surface Methodology Approach," *Cleaner Waste Systems* 12 (2025): 100379.

39. R. Roychand, S. Kilmartin-lynch, M. Saberian, J. Li, G. Zhang, and C. Q. Li, "Transforming Spent Coffee Grounds Into a Valuable Resource for the Enhancement of Concrete Strength," *Journal of Cleaner Production* 419 (2023): 138205.

40. H. A. Rondón-Quintana, F. A. Reyes-Lizcano, S. B. Chaves-Pabón, J. G. Bastidas-Martínez, and C. A. Zafra-Mejía, "Use of Biochar in Asphalts: Review," *Sustainability* 14, no. 8 (2022): 4745.

41. T. Chompoorat and S. Likitlersuang, "Influence of Asphalt Binder on Time-Temperature Shift Function for Asphalt Concrete at Large Strains," *KSCE Journal of Civil Engineering* 20, no. 7 (2016): 2765–2774.

42. S. Likitlersuang, G. T. Houlsby, and T. Chompoorat, "Model for Shear Response of Asphaltic Concrete at Different Shear Rates and Temperatures," *Journal of Engineering Mechanics* 135, no. 11 (2009): 1257–1264.

43. J. P. M. Feitosa, A. E. V. de Alencar, N. W. Filho, et al., "Evaluation of Sun-Oxidized Carnauba Wax as Warm Mix Asphalt Additive," *Construction and Building Materials* 115 (2016): 294–298.

44. A. de Bortoli, O. Rahimy, and A. Levasseur, "Environmental Life-Cycle Impacts of Bitumen: Systematic Review and New Canadian Models," *Transportation Research Part D: Transport and Environment* 136 (2024): 104439.

45. D. H. Kumar, R. K. Chinnabhandar, K. Chiranjeevi, and A. U. R. Shankar, "Effect of Aggregate Gradation and Bitumen Type on Mechanical Properties of Semi-Flexible Asphalt Mixtures," *Case Studies in Construction Materials* 18 (2023): e02025.

46. M. Bolla, M. Pettinato, V. Jankuj, J. Skrinsky, P. Perego, and B. Fabiano, "Towards the Valorization of Spent Coffee Grounds: Experimental Evaluation of Flammability and Explosion Hazards," *Journal of Loss Prevention in the Process Industries* 99 (2026): 105824.

47. R. K. Chinnabhandar, D. H. Kumar, R. G. Yatish, and A. U. R. Shankar, "Laboratory Evaluation of Use of Areca Fibres in SMA Mixes," *International Journal of Pavement Engineering* 24, no. 2 (2023): 6090.

48. A. Y. Elnour, A. A. Alghyamah, H. M. Shaikh, et al., "Effect of Pyrolysis Temperature on Biochar Microstructural Evolution,

Physicochemical Characteristics, and Its Influence on Biochar / Polypropylene Composites," *Applied Sciences* 9, no. 6 (2019): 1149.

49. M. H. Hassanjani, M. Arabani, F. M. Nejad, and M. A. Jadehkenari, "A Novel Approach to Reduce Acid Value of Waste Edible Oil Using Nano Calcium Oxide and Its Effect on Asphalt Moisture Susceptibility," *Case Studies in Construction Materials* 23 (2025): e05588.

50. M. H. Hassanjani, M. Arabani, M. M. Shalchian, and A. Amiri, "Evaluation of Different Biomass Conversion Methods to Bio-Oil for Partial Replacement of Petroleum Bitumen: Analysis of Effects and Implications," *International Journal of Pavement Engineering* 26, no. 1 (2025): 2472860.

51. P. Chindasiriphan, N. Subwilai, J. Intarasoontron, et al., "Synergistic Effects of Microencapsulated Bacterial Spores and Superabsorbent Polymer on Self-Healing Performance in Mortar," *Construction and Building Materials* 414 (2024): 135005.

52. P. Nuaklong, P. Jongvivatsakul, V. Phanupornprapong, et al., "Self-Repairing of Shrinkage Crack in Mortar Containing Microencapsulated Bacterial Spores," *Journal of Materials Research and Technology* 23 (2023): 3441–3454.

53. M. Arabani, M. Effati, M. Safari, M. M. Shalchian, and M. H. Hassanjani, "The Comprehensive Review on the Mechanisms and Performance of Different Bio-Extenders in the Bitumen," *International Journal of Pavement Research and Technology* 19, no. 2 (2026): 255–277.

54. M. Arabani, M. Sadeghnejad, J. Haghanipour, and M. H. Hassanjani, "The Influence of Rice Bran Oil and Nano-Calcium Oxide Into Bitumen as Sustainable Modifiers," *Case Studies in Construction Materials* 21 (2024): e03458.

55. M. Arabani, A. Amiri, and M. H. Hassanjani, "Utilizing Olive Pomace Oil and the Extrusion of SBS and PVC to Enhance the Physical and Rheological Characteristics of Asphalt Binder," *Case Studies in Construction Materials* 21 (2024): e04097.

56. T. Chompoorat, P. Palasing, A. Khamplod, T. Thepumong, and S. Likitlersuang, "Mechanical Properties Assessment of Corn Husk Fibre-Reinforced Cement-Treated Lakebed Sediments for Road Construction," *International Journal of Pavement Engineering* 26, no. 1 (2025): 2582734.

57. K. Hamcumpai, P. Nuaklong, P. Chindasiriphan, et al., "High-Strength Steel Fibre-Reinforced Geopolymer Concrete Utilising Recycled Granite Waste and Rice Husk Ash," *Construction and Building Materials* 433 (2024): 136693.

58. K. Hamcumpai, P. Nuaklong, P. Chindasiriphan, et al., "Enhancing High-Strength Geopolymer Concrete With Recycled Granite Aggregate Using Sugarcane Bagasse Ash and Steel Fibers," *Construction and Building Materials* 493 (2025): 143096.

59. T. Chompoorat, S. Likitlersuang, and P. Jongvivatsakul, "The Performance of Controlled Low-Strength Material Base Supporting a High-Volume Asphalt Pavement," *KSCE Journal of Civil Engineering* 22, no. 6 (2018): 2055–2063.

60. T. Chompoorat, T. Thepumong, A. Khamplod, and S. Likitlersuang, "Improving Mechanical Properties and Shrinkage Cracking Characteristics of Soft Clay in Deep Soil Mixing," *Construction and Building Materials* 316 (2022): 125858.

61. B. Punnoi, S. Arpajirakul, W. Pungrasmi, T. Chompoorat, and S. Likitlersuang, "Use of Microbially Induced Calcite Precipitation for Soil Improvement in Compacted Clays," *International Journal of Geosynthetics and Ground Engineering* 7, no. 4 (2021): 327.

62. T. Wang, H. Rong, S. Chen, et al., "TG- MS Study on in-Situ Sulfur Retention During the Co-Combustion of Reclaimed Asphalt Binder and Wood Sawdust," *Journal of Hazardous Materials* 403 (2021): 123911.

63. M. Arshad and H. M. Hamza, "Applications of Machine Learning and Traditional Prediction Techniques for Estimating Resilient Modulus Values of Unbound Granular Materials Incorporating Reclaimed Asphalt Pavement (RAP) as a Primary Component," *Construction and Building Materials* 473 (2025): 140900.

64. U. Asif, W. A. Khan, K. A. Naseem, and S. A. S. Rizvi, "Enhancing the Predictive Accuracy of Marshall Design Tests Using Generative Adversarial Networks and Advanced Machine Learning Techniques," *Materials Today Communications* 45 (2025): 112379.

65. J. Khatti, S. Mishra, A. D. Skentou, and P. G. Asteris, "Metaheuristic-Optimized XGBoost Model for Accurate Prediction of Rock Fragmentation in Mining Projects," *Transportation Geotechnics* 57 (2026): 101854.

66. J. Khatti, P. Samui, and S. Mishra, "Operational Parameter–Based Prediction of Shield TBM Advance Rate Using Explainable Computational Intelligence," 13, no. 4 (2026).

67. J. Khatti, Y. Fissha, and N. R. Cheepurupalli, "Improving End-Bearing Capacity Prediction of Rock-Socketed Shafts Using Gaussian-Augmented Optimized Extreme Gradient Boosting Models," *Scientific Reports* 16, no. 1 (2026): 1–34.

68. L. Bouaricha, J. Khatti, M. F. Yazici, A. Chehat, A. D. Henni, and L. Lancelot, "Effect of Polypropylene Fibre, Moisture Content, Relative Density, and Vertical Stresses on Mechanical Properties of Poorly Graded Sandy Soil: A Geotechnical and Hybrid XGBoost-Based Investigation," *Construction and Building Materials* 493 (2025): 143286.

69. J. Khatti, P. Samui, D. P. N. Kontoni, and P. G. Asteris, "Computational Aspects in Estimating the Bearing Capacity of RC Piles Using Hybrid Machine Learning Models," *Transportation Infrastructure Geotechnology* 13, no. 1 (2026): 773.

70. J. Zhu, B. Birgisson, and N. Kringos, "Polymer Modification of Bitumen: Advances and Challenges," *European Polymer Journal* 54 (2014): 18–38.

71. J. C. Petersen, "A Review of the Fundamentals of Asphalt Oxidation: Chemical, Physicochemical, Physical Property, and Durability Relationships," *Transportation Research Circular*no. E-C140 (2009).

72. H. Li, S. Dang, L. Liu, G. Zhang, and Z. Liu, "Valorization of Spent Coffee Grounds Into Biochar for Sustainable Asphalt Pavements: A Combined Molecular Dynamics and Experimental Study," *Construction and Building Materials* 511 (2026): 145314.

73. S. Girimath, D. Singh, and B. Showkat, "Influence of Bio-Oil Modification on Moisture-Induced Damage Potential of Asphalt Binder and Mix," *Advances in Civil Engineering Materials* 10, no. 1 (2021): 276–299.